Mineral Recovery Enhanced Desalination (MRED) Process: An Innovative Technology for Desalinating Hard Brackish Water

Authors:

Bruce M. Thomson (corresponding author), bthomson@unm.edu, Dept. of Civil, Construction & Environmental Engineering, MSC01-1070, University of New Mexico, Albuquerque, NM 87131
Sugam Tandukar, sugam.tandukar@woodplc.com, Wood Technical Consulting Solutions, Albuquerque, NM
Ayush Shahi, ayush.raj.shahi.ars@gmail.com, Dept. of Environmental and Architectural Engineering, University of Colorado, Boulder, CO
Carson Odell Lee, carl@unm.edu, Dept. of Civil, Construction & Environmental Engineering, University of New Mexico, Albuquerque, NM
Kerry J. Howe, howe@unm.edu, Dept. of Civil, Construction & Environmental Engineering, University of New Mexico, Albuquerque, NM

Abstract

Desalination of water containing high concentrations of calcium, dissolved carbon dioxide, sulfate, silica and other sparingly soluble salts is difficult because of the scaling potential. An innovative pre-treatment scheme was investigated at bench scale that selectively removes these constituents and produces a soft water to enable desalination with high feed water recovery. The process first removes dissolved carbon dioxide by air stripping at low pH. Magnesium is removed by precipitation at high pH. Calcium is removed by ion exchange (IX), and sulfate is removed by nanofiltration (NF). Cation regenerant from IX, containing calcium, and concentrate from NF, containing sulfate, is combined to precipitate gypsum. Concentrate from the desalination process consisting of a concentrated NaCl solution is used to regenerate the IX resins. The selective precipitation, IX, and NF processes were tested in laboratory experiments and produced magnesium hydroxide and gypsum at greater than 90% and 95% purity respectively. A process model was developed to calculate process performance, mass and liquid flow rates. The MRED process offers the following benefits: 1) greater recovery of brackish feedwater by a desalination process, 2) recovery of marketable commodities and 3) reduction in the volume and mass of waste products from the treatment process.

Keywords: brackish water desalination, scale forming potential, pretreatment, selective precipitation

Highlights

- A novel pretreatment process to improve desalination of hard brackish water.
- Uses well known existing unit operations to achieve innovative objectives.
- Recovery of high purity commodity materials including magnesium hydroxide ($Mg(OH)_2$) and gypsum ($CaSO_4 \cdot 2H_2O$) from hard brackish water.
- Reduced mass and volume of desalination concentrate requiring disposal

Graphical Summary

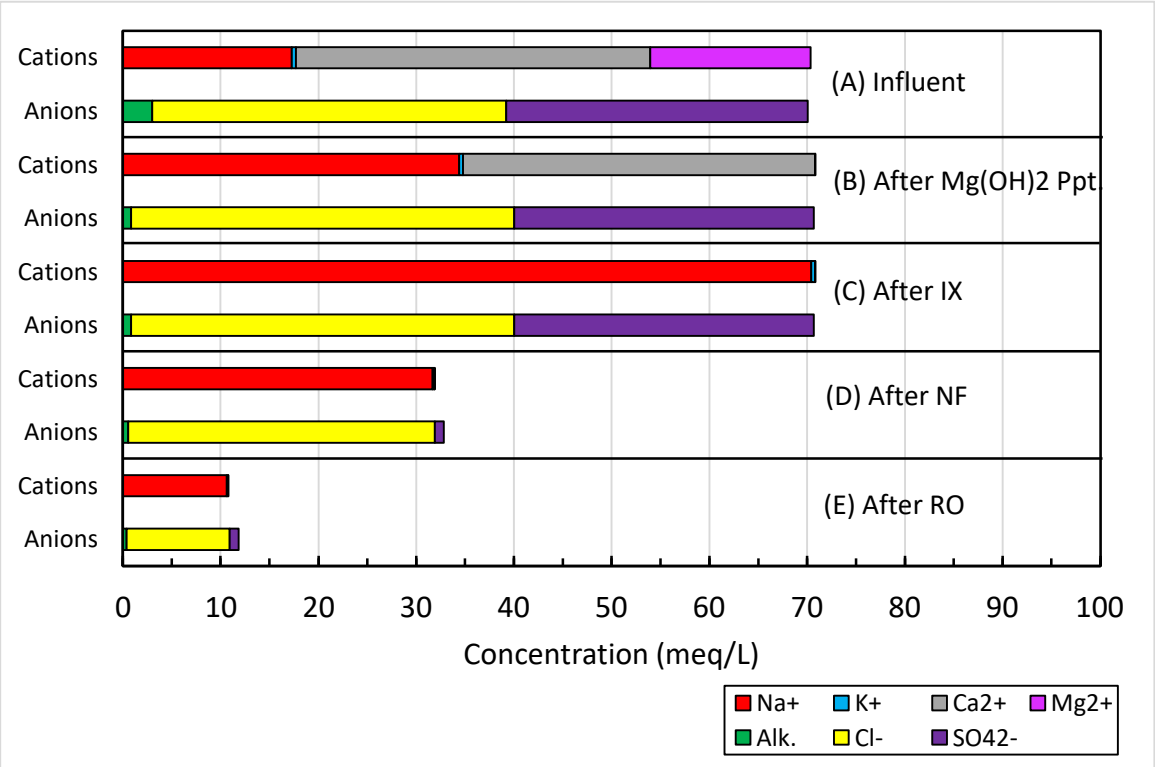

1 Introduction

As demand for sources of fresh water for potable and industrial use increases, water managers are increasingly interested in lower quality water that may be purified through advanced treatment processes to a sufficient quality that will allow it to augment existing supplies (Ziolkowska and Reyes, 2017). Two sources of low quality water that are of current interest are municipal and industrial wastewater, and brackish (total dissolved solids concentration (TDS) less than 10,000 mg/L) and/or highly saline water (TDS concentration greater than 10,000 mg/L).

In contrast to wastewater reuse, which is at least conceptually possible anywhere that wastewater is generated, interest in developing brackish and saline water resources is site specific and limited to locations where such sources are available. Often these locations are in arid parts of the world where the high demand for water and lack of freshwater resources may justify the high costs of desalination. Opportunities for developing brackish/saline water resources as a source of water supply have been identified (Nashed et al., 2014; Allam et al., 2003; Talaat et al., 2003; Hadadin et al., 2010; Jaber and Mohsen, 2001; Altaf et al., 1993; Ziolkowska and Reyes, 2017; Ruiz-Garcia and Feo-Garcia, 2017).

Coastal communities often evaluate seawater as a source of supply (Ziolkowska and Reyes, 2017) whereas inland communities are generally limited to consideration of brackish groundwater. The United States Geological Survey (USGS) (Stanton et al., 2017; Stanton and Dennehy, 2017) has a national program to identify brackish groundwater resources. In the arid southwestern U.S., studies of brackish groundwater resources have been performed in Texas (EPWU, 2020; TWDB, 2018 and Kalaswad et al., 2005) and New Mexico (NMBGMR, 2018 and Newton and Land, 2016).

Development of inland brackish water resources has both regulatory and technical challenges that are different than desalinating seawater at coastal locations. The policy and regulatory issues usually concern the ownership of the water and the rights to develop it and have been discussed by Buono et al. (2016). The technical challenges include the high concentrations of scale forming minerals and limited options for disposal of waste salts (Thomson and Howe,

2009; McMahon et al., 2015; Stariha et al., 2014). The importance of pre-treating the feed water prior to any desalination process cannot be overstated. A review of fouling mechanisms has been provided by Ruiz-Garcia et al. (2017) and a recent review of pre-treatment methods has been provided by Anis et al. (2019).

The objective of this bench-scale experimental testing and modeling research was to investigate the technical feasibility of a novel process to pre-treat hard brackish water prior to desalination that addresses both technical challenges. The process was developed to treat flue gas desulfurization (FGD) wastewater from coal fired electric power plants but it can treat any hard brackish water. The process recovers the commodity minerals magnesium hydroxide ($Mg(OH)_2$) and gypsum ($CaSO_4 \cdot 2H_2O$). Removing scale forming minerals from the water enhances the feed water recovery by a subsequent desalination process is facilitated. Greater than 90% of the feed water can be recovered and, depending on the feed water chemistry, the waste product is a brine consisting mostly of sodium (Na), potassium (K), and chloride (Cl). Based on these attributes, this process has been called the Mineral Recovery and Enhanced Desalination (MRED) process (Thomson et al., 2019). The benefits of the MRED process are increased recovery of feed water by reducing scaling potential of the desalination process, and though the value of these minerals is not large, their recovery reduces the cost of waste management and disposal. It will also provide a consistent feed water quality to the subsequent desalination process that will facilitate its optimal operation (Ruiz-Garcia et al., 2020). The MRED process can improve the performance of any membrane or thermal desalination technology and is not specific to reverse osmosis (RO) or other desalination methods.

2 Theoretical Considerations

2.1 Description of the MRED Pre-Treatment Process

The unit operations in the MRED process remove high purity minerals that have commodity value. Each unit operation is based on well-understood chemical and engineering principles, although investigating the effect of high ionic strength was an important objective in the laboratory research.

A diagram of the MRED process is presented in Fig. 1. A summary of each operation follows.

Degasification. An acid, such as hydrochloric acid (HCl), is added to reduce the pH to ~4.5 to remove alkalinity, and the feed solution is treated by air stripping to remove dissolved CO_2. Carbonate removal prevents subsequent formation of carbonate precipitates, especially $CaCO_3$ which reduces scaling of membrane or heat transfer surfaces and improves the purity of recovered magnesium hydroxide and gypsum. Air stripping will assure that the water fed to subsequent unit operations is highly aerated. Removal of alkalinity will also reduce acid and base requirements for subsequent pH adjustment.

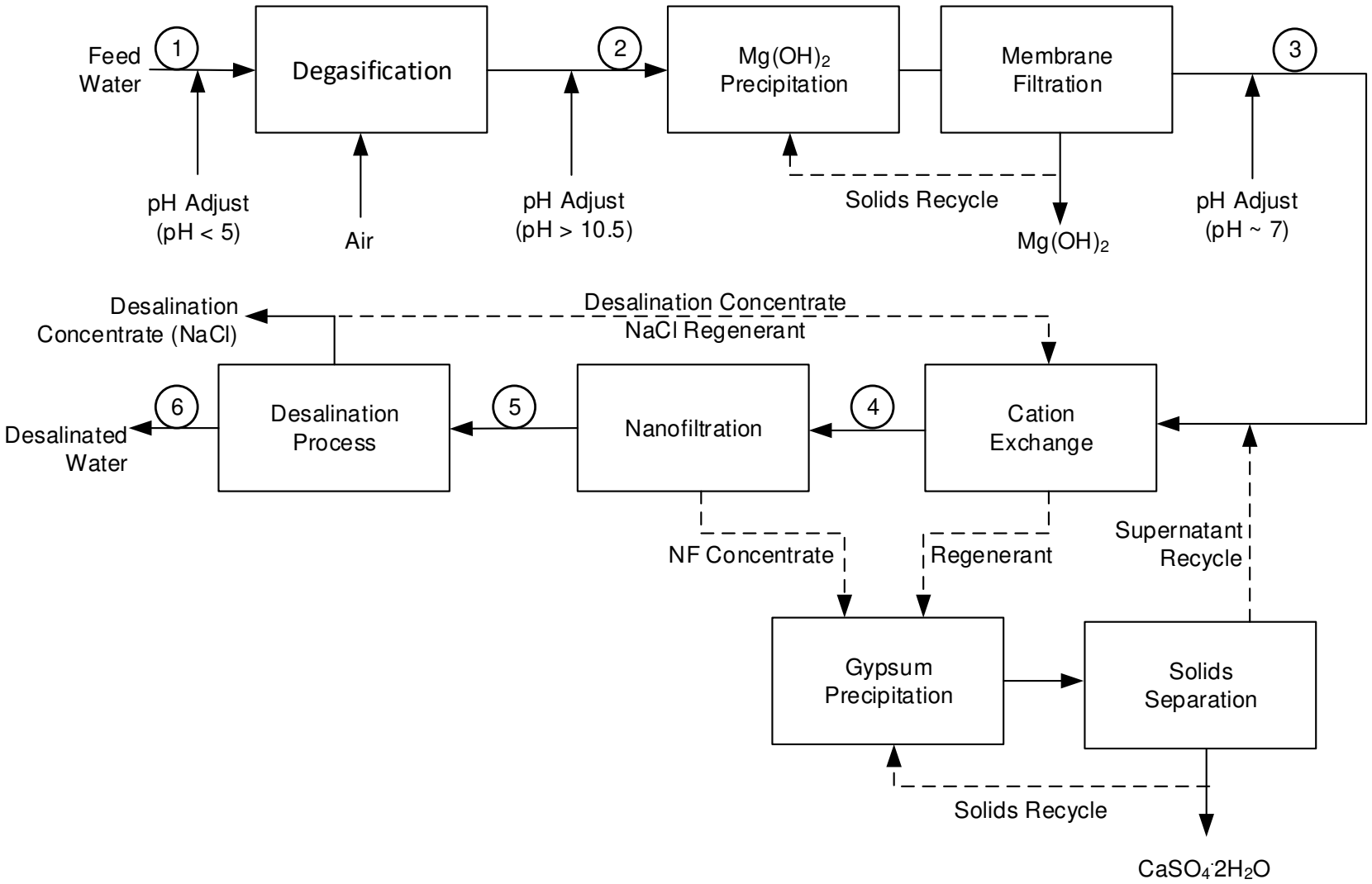

117

118 Fig. 1. Flow diagram of the Mineral Recovery Enhanced Desalination (MRED) process.

119

Magnesium Hydroxide Precipitation: The pH is raised to 10.5 – 11.5 using NaOH to precipitate magnesium hydroxide. This step will also remove dissolved silica (SiO_2), and most transition metals. Precipitation occurs in a mixed reaction vessel and solids, including colloidal material, are removed by membrane filtration. Solids recycle may be included to increase the performance of the precipitation process.

Cation Exchange: Following magnesium hydroxide precipitation, the remaining dominant polyvalent cation in solution is calcium, though strontium and barium might be present in low concentrations. Cation exchange will selectively remove calcium and other remaining divalent cations by exchanging with sodium. After IX the solution consists of sodium cations and anions dominated by chloride and sulfate. The IX resin is regenerated using the concentrated NaCl brine from the desalination unit, which eliminates the need to purchase salt.

Nanofiltration: The nanofiltration (NF) process removes sulfate from solution. Nanofiltration membranes selectively retain polyvalent ions in the feed solution, which are concentrated in the concentrate stream. Since calcium, magnesium, other metals and dissolved carbon dioxide are removed prior to the NF step, the only polyvalent ion present in solution is sulfate. Therefore, the NF process is not subject to mineral scaling and can be operated at a high feed water recovery.

Gypsum Precipitation: The regenerant brine from the IX process containing a high calcium concentration is combined with the concentrate from the NF process which has a high sulfate concentration. Mixing the two streams will precipitate gypsum. Gypsum solids are removed by sedimentation. The supernatant from the gypsum precipitation process consists of a NaCl solution and saturated concentrations of calcium and sulfate due to the relatively high solubility of gypsum. The supernatant is recycled back to the IX process for further recovery of water, calcium and sulfate.

Desalination: The final step in the MRED process is desalination. The feed water to the desalination process consists of a NaCl solution with negligible potential for scale formation. The low scale formation potential allows high recovery of the feed water, less scaling, and easier cleaning of process equipment. Some of the concentrate from desalination is used to regenerate the IX resins. The brine may have value as salt for industrial processes, or it could simply be disposed of as concentrated brine.

The research described in this paper investigated selective precipitation and membrane filtration of magnesium hydroxide, removal of calcium by IX, selective removal of SO_4^{2-} by NF, and selective precipitation of gypsum at bench scale. The experimental results were used to develop a mass balance model of the MRED process to simulate process performance.

2.2 Theoretical Considerations Related to High Ionic Strength Solutions

The performance of a process for pre-treating hard brackish water prior to desalination is complicated due to its high ionic strength and near saturation conditions for common scale forming minerals. Ionic strength is a measure of the total ionic composition of a solution and is calculated as:

$$I = \frac{1}{2} \sum_{all\ ions} [i]\, z_i^2 \qquad (1)$$

Where $[i]$ is the molar concentration of ionic species i and z_i is its charge.

Note that since I is calculated using the square of the charge of each ion it is not proportional to total dissolved solids (TDS) concentration but also depends on solution chemistry. It is possible to have a comparatively low TDS water with high concentrations of polyvalent ions that has a higher I than a higher TDS water containing only sodium and chloride. Ionic strength is important because it affects the activity coefficient of ionic constituents. The value of the activity coefficient of a dissolved molecule depends on its chemistry in aqueous solution, particularly its charge (Benjamin, 2015). A plot of the activity coefficient versus I for major ions in brackish and saline water is presented in Fig. 2. The values of activity coefficients for

common cations and anions in hard water were calculated using the Truesdell-Jones extension of the Debye-Huckel equation. This equation is valid up to I ~ 2.5 M and is appropriate for modeling brackish and saline water chemistry (Benjamin, 2015; Langmuir, 1997). For reference, the ionic strength of seawater is 0.7 M. The effect of I on solubility and precipitation reactions is especially important to the MRED process. The Truesdell-Jones equation and the constants used to calculate the activity coefficients shown in Fig. 2 are presented in Appendix I.

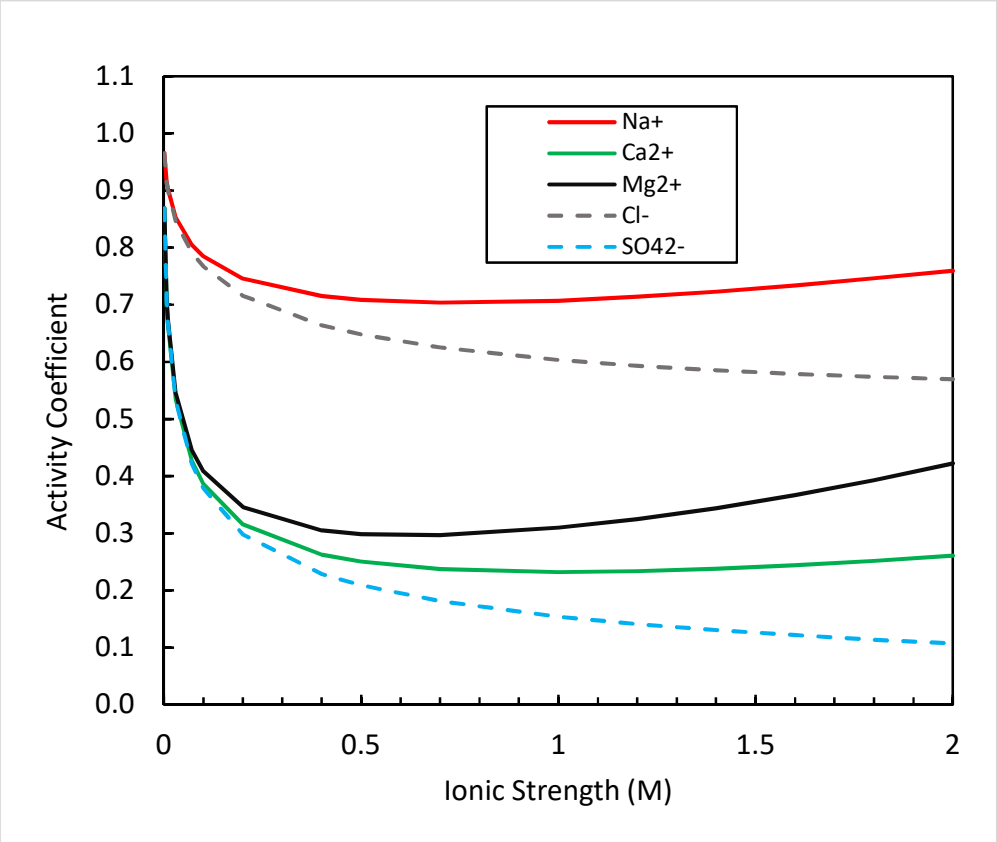

Fig. 2. Effect of ionic strength on the activity coefficients of major ions present in brackish and saline as a function of ionic strength (I) calculated using the Truesdell-Jones model.

Solubility Considerations

The most common solid phases of concern when desalinating hard brackish or saline water are carbonates such as calcite ($CaCO_3$), calcium fluoride (CaF_2), sulfates such as gypsum ($CaSO_4 \cdot 2H_2O$) and barite ($BaSO_4$), and silica (SiO_2) (Howe et al., 2012). The solubility of some of these solids as a function of pH at T = 25 °C, I = 0 M and I = 0.2 M is presented in Fig. 3.

Magnesium hydroxide is included in this diagram as it is removed as a precipitate in the MRED process. Strontium and barium are two other constituents that are present at trace levels in seawater but may be found at problematic concentrations in groundwater. They form even less soluble sulfate precipitates than calcium and thus would be readily removed by the MRED process. This plot illustrates the marked effect that I has on the solubility of salts composed of two divalent ions such as gypsum and calcite; their solubility increases by nearly an order of magnitude at I = 0.2 M.

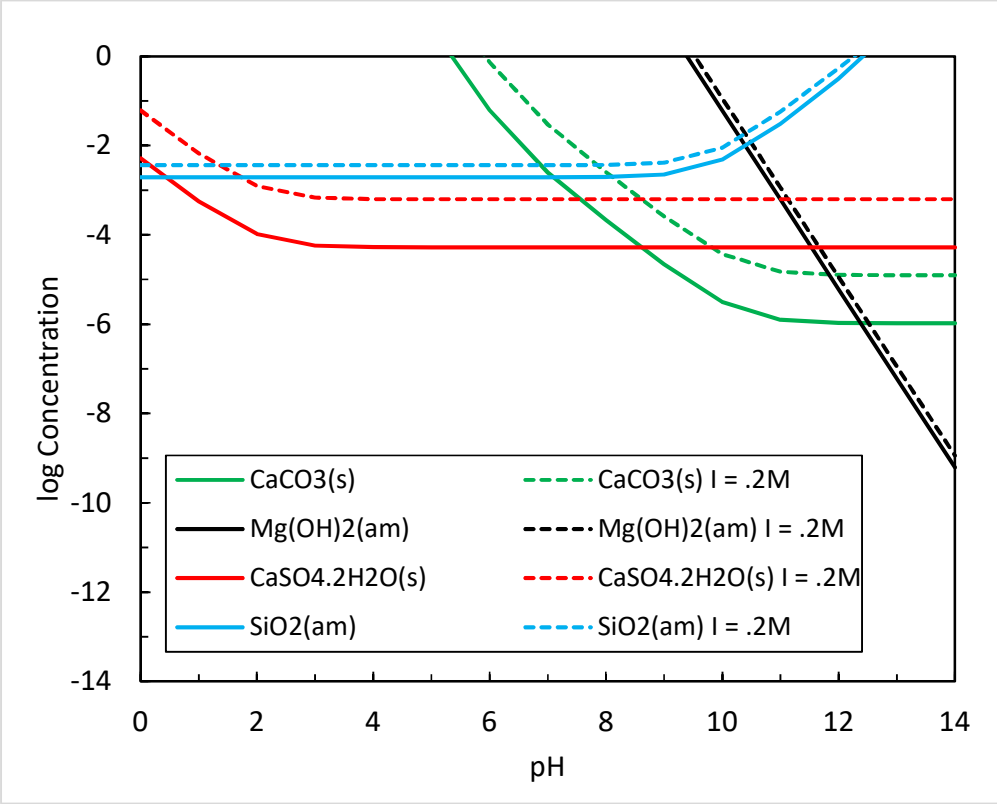

Fig. 3. Solubility of gypsum ($CaSO_4.2H_2O$), calcite ($CaCO_3$), amorphous $Mg(OH)_2$ and amorphous SiO_2 at T = 25 °C in water at I = 0 M (solid lines) and I = 0.2 M (dashed lines). The concentration of total dissolved CO_2 is 0.003 M and that of the total dissolved SO_4^{2-} is 0.5 M. The log of the molar concentrations of Ca, Mg, and SiO_2 are plotted on the y-axis. Thermodynamic data are from Stumm and Morgan (1996).

Two of the constituents of brackish and saline water, magnesium hydroxide and gypsum, have value as commodity products if they can be recovered at sufficient purity. Magnesium hydroxide is used as an antibacterial agent, acid neutralizer, paper preservative, chemical sensor

for ethanol, component for membranes, and as a flame retardant (Pilarska et al., 2017). It occurs as the mineral brucite ($Mg(OH)_{2(s)}$) in nature.

Gypsum is used in wallboard and as soil amendment. As shown in Fig. 3, gypsum solubility is largely independent of pH over the range of pH 3 to 14 because the gypsum precipitation reaction does not involve hydrogen ions (H^+). Ben Ahmed (2014) showed that at I > 0.3 M high concentrations of magnesium will decrease the solubility of gypsum by up to 12% but will also decrease its purity, thus, magnesium is removed before calcium in the MRED process.

2.3 Ion Exchange (IX)

Strong acid cation exchange resins are commonly used for water softening. The exchange reaction for removal of calcium can be written as follows where R represents exchange sites on the resin.

$$2(R\text{-}Na) + Ca^{2+} = R_2\text{-}Ca + 2Na^+ \quad (2)$$

Water is fed to a column containing IX media and flows through until all exchange sites on the media are occupied by calcium ions (i.e. the media is exhausted). After the column reaches exhaustion, the media is regenerated by passing a few bed volumes (BVs) of concentrated salt brine (NaCl) through the column to replace calcium on exchange sites with sodium ions (Sengupta, 2017; Clifford et al, 2011).

The performance and design of an IX process depends on two characteristics of the resin; its selectivity and its capacity. The selectivity of a resin is its preference for one ion over another. Cation exchange resins used in water softening prefer calcium and magnesium over sodium because IX resins prefer polyvalent ions over monovalent ions in low I water (Sengupta, 2017; Clifford et al., 2011).

Resin capacity is the total amount of ionic constituents that can be contained on the resin and is usually measured in units of meq/g or meq/mL. The capacity is based on the surface area and

number of exchange sites on the resin surface and is determined by the chemical formulation for the resin developed by its manufacturer.

The binary separation factor ($\alpha_{Na/Ca}$) (Clifford et al., 2011) is used to characterize a resin's selectivity and is defined as:

$$\alpha_{Ca/Na} = \frac{\text{distribution of Ca between phases}}{\text{distribution of Na between phases}} = \frac{y_{Ca}/x_{Ca}}{y_{Na}/x_{Na}} \quad (3)$$

Where y_{Ca} and y_{Na} are the equivalent fractions of calcium and sodium respectively in the resin and x_{Ca} and x_{Na} are the equivalent fractions of calcium and sodium respectively in the solution. The binary separation factor can be written in terms of concentrations in solution and resin phases as:

$$\alpha_{Ca/Na} = \frac{q_{Ca}\, C_{Na}}{C_{Ca}\, q_{Na}} \quad (4)$$

Where q_{Ca} and q_{Na} are the ionic concentration of calcium and sodium in the resin (eq/L) and C_{Ca} and C_{Na} are ionic concentrations of calcium and sodium in solution (eq/L). High values of $\alpha_{Ca/Na}$ mean the resin is more selective for calcium than sodium.

The resin selectivity changes at high I due to the decreased activity coefficient of polyvalent ions compared to monovalent ions (Fig. 2) and will result in reversal of these selectivity sequences. Selectivity reversal improves the regeneration process as the high I causes preference for sodium ions over calcium, and the very high sodium concentration drives the reaction represented by equation (2) to the left. Salt concentrations ranging from 5% to saturation (>35%) are used for regeneration (Clifford et al., 2011).

In practice, most ion exchange is performed using columns packed with resin beads and operated in a down-flow orientation. The performance of an IX column is usually measured as the number of BVs of water that can be treated prior to exhaustion of the media.

2.4 Nanofiltration

Nanofiltration (NF) is used to preferentially remove polyvalent ions from water. NF is a separation process in which monovalent ions diffuse through a membrane faster than polyvalent ions (Howe et al., 2012; Oatley-Radcliff et al. 2017).

The three important performance criteria for membrane processes are rejection, flux, and feed water recovery. Sulfate rejection by NF membranes ranges from 92% to greater than 99% based on the type of membrane used and the pressure applied whereas chloride rejection is much less because it is a monovalent ion and therefore diffuses more readily through the membrane (Kosutic, 2004).

3 Research Methods

The research focused on the performance of key unit operations of the MRED process that are especially uncertain in high ionic strength solutions. These processes were selective precipitation of magnesium hydroxide, IX removal of calcium, NF removal of sulfate, and selective precipitation of gypsum. All experiments were conducted at room temperature which was approximately 21 °C

3.1 Batch Experiments to Evaluate Mg $(OH)_2$ Precipitation

Batch precipitation experiments were conducted to measure precipitation and determine the purity of Mg $(OH)_2$, precipitated at high pH from low, medium and high TDS brackish water solutions. Three simulated hard brackish/saline water solutions were prepared using reagent grade chemicals and deionized (DI) water. Table 1 presents the composition for these waters. These solutions are based on the chemistry of actual FGD wastewaters from coal fired electric power plants. Note that these solutions had low alkalinities as would be achieved following acidification and removal of dissolved CO_2.

Batch precipitation experiments were performed in triplicate. Fifty mL of solution was pipetted into Erlenmeyer flasks, each flask was set on a magnetic stirrer, and the pH was raised using

301 reagent grade NaOH to reach a target pH. For the magnesium hydroxide precipitation
302 experiments the target pH values were 10.5, 11.5, and 12.5. After the initial pH was achieved,
303 the solution was transferred to a 50 mL capped plastic vial, and the solids were allowed to settle
304 overnight.

305

306 Table 1. Simulated brackish water composition for low, medium, and high TDS solutions.

Constituent	Low TDS Soln.		Medium TDS Soln.		High TDS Soln.	
	(mg/L)	meq/L	(mg/L)	meq/L	(mg/L)	meq/L
Na^+	398	17.3	2,540	110.4	6,680	290.4
Ca^{2+}	725	36.3	659	33.0	4,240	212.0
Mg^{2+}	199	16.4	534	44.0	2,830	232.9
Cl^-	1,290	36.2	3,380	95.2	24,300	684.5
SO_4^{2-}	1,480	30.8	4,340	90.4	2,180	45.4
Alkalinity*.	151	3.0	100	2.0	274	5.5
TDS	4,290		11,600		40,500	
Ionic Strength (M)	0.09		0.21		0.96	

307 *Alkalinity is in units of mg $CaCO_3$/L

308

309 Following settling, the solutions were filtered through 0.45 μm pore diameter Supor-450
310 membrane filters. The filtrate was transferred to a sealed sample vial and refrigerated. Selected
311 filters containing the dried precipitates were weighed to measure the TSS and then were
312 dissolved in 2% nitric acid for cation analysis to determine the purity of the solids. The
313 remaining samples were stored in sealed containers for analysis by XRD and SEM.

314

315 ### 3.2 Removal of Solids Following $Mg(OH)_2$ Precipitation

316 Batch experiments were conducted to determine the settling characteristics of the solids from the
317 batch precipitation experiments. A slurry of precipitated $Mg(OH)_2$ was placed in a 0.5 m tall
318 column and allowed to settle. The height of the solids interface was measured with time. The

settling experiments found that the magnesium hydroxide solids settled poorly therefore, a series of experiments were performed using a lab scale membrane filtration system. A $Mg(OH)_2$ suspension was prepared in an 80 L plastic container and circulated through a 6 foot long PVC membrane module containing a Porex TMF 1.05 tubular membrane with a nominal pore size of 0.1 μm and a total surface area of 0.07 m^2 (item number MMV2S0160VC). A Little Giant 3E-34N Dual Purpose Small Submersible Pump was used for recirculation. The initial flowrate was 15 L/min to produce a cross flow velocity of 2 m/s.

The system was cleaned by circulating 1% citric acid through the system for an hour and rinsing with tap water, a common cleaning procedure for NF and other membranes. 20 L of brackish water was prepared with water chemistry as shown in Table 1 and the pH was raised to 11.5 using 10M NaOH. The solids were retained in the system while the permeate was discarded, thus, the solids concentration in the feed water increased during the filter run. The system was run for 90 minutes or until all of the water was treated. Samples were taken every 5 minutes from the permeate and feed water tank and the turbidity and TSS were measured. If the turbidity of the sample was above 1000 NTU, samples were diluted 1:10. The permeate and recirculation flow rates, and feed pressure, and temperature in the feed tank were recorded each time samples were collected. Membrane filtration tests were done for low and medium TDS brackish water.

After each filter run, the membrane filter was backwashed with tap water for two to three minutes and the feed tank was filled with a new batch of water. The filtrate flux was calculated by dividing the permeate flow rate by the membrane area. Specific flux was calculated by dividing the standard flux by pressure.

For the last set of experiments, the filtrate was returned to the feed tank without backwash or chemical cleaning to measure performance at a constant TSS concentration.

3.3 Ion Exchange Experiments

Batch cation exchange experiments were conducted to determine the effect of I on binary separation factors. Two resins were used, Purolite SSTC60 with an exchange capacity of 3.04

eq/L and Dow Amberlite HPR 1300 with an exchange capacity of 2.2 eq/L. The exchange sites were placed in the sodium form by soaking them in a 10% by mass NaCl solution for 24 hours.

Batch IX experiments were conducted in 50 mL Erlenmeyer flasks at initial I concentrations of 0.01 M, 0.1 M and 1.0 M. The solutions were prepared using NaCl and $CaCl_2$ salts. Solutions of varying ratios of calcium to sodium were prepared at each value of I and weighed amounts of resin were added. Varying masses of resin were added so that measurable concentrations of the cations would be present in solution after the system reached equilibrium. The flasks with solutions were placed on a shaker table for 24 hours and the initial and final concentrations of calcium and sodium were measured.

IX column experiments were done to determine the number of BVs of water that could be treated to reach exhaustion for solutions of varying I, and to determine if exchange capacity was lost over multiple exchange-regeneration cycles.

Glass columns, 2.5 cm diameter by 15 cm long, were filled with resin and glass wool was placed at the top and bottom to support the resin and distribute flow across the column width. A flow of 10.13 mL/min was selected to establish a 5 minute empty bed contact time (EBCT) using a Masterflex C/L Digital Microflex Pump System. Five BVs of 10% NaCl solution were passed through the columns to place the resin in the sodium form followed by two BVs of rinsing with deionized water. Low, medium and high I water was passed through the columns and samples were collected every two to five BVs for analysis by ICP-OES. Three exchange-regeneration cycles were performed.

The composition of feed water used in the IX column studies is presented in Table 2. Note that no magnesium was present as it would be previously removed by magnesium hydroxide precipitation.

3.4 Nanofiltration Experiments

Nanofiltration (NF) removal of sulfate for low and medium TDS solutions was first modeled using the WAVE software (Dow Water & Process Solutions, 2019). The WAVE model uses the

feed water composition, the number of NF treatment stages, the NF membrane characteristics, and the design parameters of interest. Modeling was done for two, three and four stage NF systems using the Dow Filmtec NF-270-400-34i membrane (now marketed by Dupont). The WAVE model predicts fractional feed water recovery of the NF system, permeate and concentrate flow rates, and rejection of dissolved ions.

Table 2. Chemical composition of simulated hard brackish or saline water used in the IX column experiments. Magnesium is not included because it was previously removed by high pH precipitation.

	Concentration (meq/L)		
Constituent	Low TDS Soln.	Medium TDS Soln.	High TDS Soln.
Na^+	59.4	278.	682.0
Ca^{2+}	36.3	165.	223.0
Cl^-	65.1	165.	882.0
SO_4^{2-}	30.8	277.	22.6
TDS (mg/L)	5,900	28,800	52,500
Ionic Strength (M)	0.13	0.66	1.03
$C_{Na}/(C_{Na} + C_{Ca})$	0.65	0.55	0.76

A bench scale NF system was used to confirm the rejection of major ions by Dow Filmtec NF 270 membranes, a commercially-available membrane designed for high rejection of divalent ions while achieving lower rejection of monovalent ions. A 160 cm^2 flat sheet of this membrane material was placed in a custom-designed polypropylene flat-sheet membrane cell that has been described previously (Farias et al., 2014), and water was circulated at a flow of 1,732 mL/min using a high pressure pump. Pressure was controlled by a needle valve and was adjusted to maintain a desired feed pressure which was continuously monitored. Feed pressures between 5.5 and 13.5 bar (80 to 195 psi) were used depending on the I of the solution (see Table 3). The permeate flow rate was determined by measuring the time to fill a 10 mL graduated cylinder. Both permeate and concentrate flows were returned to the feed reservoir.

Brackish water of low and medium TDS were used in the NF experiments and was prepared using reagent grade NaCl and Na_2SO_4 (Table 4). Operating conditions are summarized in Table

3. Twenty liters of the simulated brackish and saline water was prepared. Samples of the feed water, permeate and concentrate were collected and analyzed for pH, electrical conductivity, and major ion chemistry. The system was run for at least one hour to allow it to stabilize, and samples were collected at 0, 30 and 60 minutes after the stabilization period.

Table 3. Experimental parameters for nanofiltration (NF) experiments.

Membrane	DOW NF 270
Feed Pressure (psi)	80, 105, 130 (low TDS) 145, 170, 195 (medium TDS)
Feed Flow Rate (mL/min)	1,732
Temperature (◦C)	25
Spacer Thickness (mil)	31

Table 4. Composition of brackish water used in NF experiments.

Ions	Low TDS Soln. (mg/L)	Medium TDS Soln. (mg/L)
Na^+	1,600	4,460
Cl^-	1,290	3,610
SO_4^{2-}	1,480	4,340
Ionic Strength (M)	0.082	0.223

3.5 Gypsum Precipitation Experiments

Gypsum precipitation experiments were conducted using simulated IX regenerant and NF concentrate at neutral pH. The purpose was to measure the quantity and purity of solids produced, solids settleability, and the chemistry of the supernatant. The composition of the simulated IX regenerant was similar to that from a resin regenerated with two BVs of 10% NaCl solution. The fraction of exchange sites occupied by calcium ions varied depending on I of the solution and was measured in the batch IX experiments. These experiments found The binary

separation factors measured in the batch IX experiments were used to calculate that 51% of the exchange sites were occupied by calcium for the low TDS solution, 42% for the medium TDS solution and only 15% of the sites were filled by calcium for the high TDS solution. Because so little calcium was retained on the resin in the high TDS IX experiments, no gypsum precipitation experiments were done for this solution. A summary of the composition of IX regenerant for regenerant solutions from the low TDS and medium TDS experiments is presented in Table 5.

The composition of the simulated NF concentrate was determined from the manufacturer's specifications for the NF membrane. A 90% feed water recovery was assumed along with 50% chloride rejection and 96% sulfate rejection. The sodium concentration in the concentrate was calculated to give an ion balance in the solution. The composition of the simulated NF concentrate and the IX regenerant is presented in Table 5. The lower calcium concentration in the medium TDS regenerant compared to the low TDS regenerant is due to less calcium removal by the IX resins in the medium TDS solution. Note that the IX regenerant includes 2,130 mg/L of magnesium. Magnesium was added to the recipe after early $Mg(OH)_2$ precipitation experiments had high residual magnesium concentrations. Subsequent experiments (after the medium TDS gypsum precipitation experiments were complete) found complete Mg removal but the experiments were not repeated since, as will be shown in Section 4.2, it had no measurable effect on gypsum precipitation.

Gypsum precipitation was accomplished by mixing solutions of the simulated IX regenerant and NF concentrate in duplicate experiments. 25 mL of each of these solutions was added to an Erlenmeyer flask, the pH was recorded, and the solutions were agitated overnight. The solutions were filtered through 0.45 μm membrane filters which were dried at 65 °C, and weighed to determine suspended solids concentration. The lower drying temperature was used to prevent loss of waters of hydration from the gypsum precipitate. One filter containing the precipitate was dissolved in 2% nitric acid for the cation analysis by ICP-OES, and the other sample was used for solids analysis by XRD and SEM. The filtrate was analyzed for cations by ICP-OES and for anions by IC.

Table 5. Composition of simulated NF concentrate and IX regeneration solution for low TDS and medium TDS waters.

	NF Concentrate		IX Regenerant	
Ion	Low TDS Soln. (mg/L)	Medium TDS Soln. (mg/L)	Low TDS Soln. (mg/L)	Medium TDS Soln. (mg/L)
Na^+	11,500	32,900	21,300	24,400
Ca^{2+}	0	0	15,500	9,260
Mg^{2+}	0	0	0	2,130
Cl^-	7,070	19,900	60,300	60,300
SO_4^{2-}	14,300	41,800	0	0
Alk.*	150.	100.	122.	122.
Ionic Strength (M)	0.57	1.57	2.31	2.03

*Alkalinity in units of mg $CaCO_3$/L

3.6 Analytical Methods

All experiments were performed in the Environmental Engineering Labs at the Department of Civil, Construction and Environmental Engineering, University of New Mexico (UNM). Cations were analyzed by Inductively Coupled Plasma – Optical Emission Spectroscopy (ICP-OES) using Perkin Elmer Avio 500, and Perkin Elmer Optima 5300 DV instruments (Method 3120, Standard Methods, APHA et al., 2018). Anions were analyzed by ion chromatography (IC) using a Dionex ICS 1100 Ion Chromatography (IC) instrument (Method 4110, Standard Methods, APHA et al., 2018). A TESCAN VEGA3 Scanning Electron Microscope - Energy Dispersive Spectroscopy system (SEM-EDS) was used to determine the elemental composition of solids from precipitation experiments. The SEM image, elemental spectrum charts, and quantitative analysis tables were recorded. A Rigaku ZSX Primus II X-Ray Diffractometer (XRD) was used to identify the mineral phase of the solids from the precipitation experiments. The peaks were matched automatically by JADE software (the software to operate the XRD

467 instrument). After analyzing the peaks, a quantitative analysis was performed, and the
468 composition of mineral phases in % mass basis was obtained.
469
470 pH was measured using a calibrated pH meter (Method 4500-H^+, Standard Methods, APHA et
471 al., 2018). Turbidity was measured using a Hach 2100P turbidimeter (Method 2130, Standard
472 Methods, APHA et al., 2018). Total suspended solids (TSS) was measured by filtering solutions
473 through membrane filters, drying the filter at 105 °C and weighing (Method 2540, Standard
474 Methods, APHA et al., 2018)

475 4 Experimental Results

476 4.1 Mg $(OH)_2$ Precipitation

477 Laboratory experiments were conducted to measure the quantity and purity of magnesium
478 hydroxide precipitated from simulated brackish water at pH values of 10.5, 11.5, and 12.5 (Fig.
479 4). At a pH near 11.5, greater than 95% magnesium removal was achieved in the low TDS and
480 high TDS solution and 84% removal from the medium TDS solution. Little removal of sodium
481 was found. Greater than 95% magnesium removal was achieved at pH ≥ 10.5 in all solutions
482 except the low TDS solution, and greater than 98% magnesium removal was measured for all
483 solutions at pH ≥ 11.5.
484

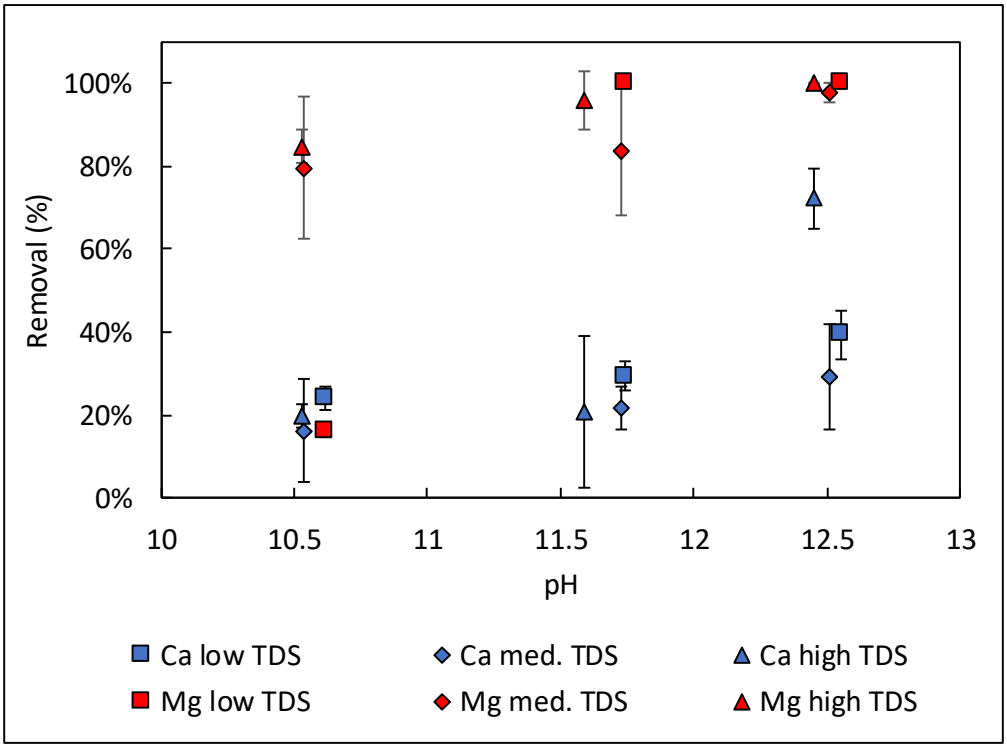

Fig. 4. Percent removal of calcium and magnesium as a function of pH at low, medium and high TDS concentrations. Error bars show the standard deviation of triplicate results.

The final concentration of the cations in the filtrate is presented in Table 6 and shows that nearly complete removal of magnesium from solution was achieved at pH ≥ 11.5 in agreement with the graphical summary shown in Fig. 3 as well as geochemical calculations done with PHREEQC (Parkhurst and Appelo, 2013). High purity $Mg(OH)_2$ precipitates were obtained by raising the pH of the solutions to pH 11.5 and above after removal of dissolved CO_2. Elemental analysis of the precipitates found that magnesium accounted for nearly 90% or more of the metals in the precipitate (Table 6) from the medium and high TDS brackish water solutions. The lower magnesium purity precipitated from the low TDS solution is believed to be due to errors associated with collecting, dissolving, and analyzing the small amount of solid precipitated from this solution. Near pH 12.5, elevated concentrations of calcium were found in the precipitates, which may be due to formation of carbonate phases as atmospheric CO_2 was absorbed into the solution at this pH. The high purity of the solids summarized in Table 6 are consistent with the results measured by SEM-EDS discussed below.

An elemental analysis of the precipitate from the medium TDS solution at pH 11.7 by SEM-EDS found 37.4% magnesium, 7.57% calcium, 45.5% oxygen, and 7.81% carbon on a mass basis. Trace amounts (< 1%) of sodium, sulfur, and chloride were also detected. Thus, magnesium accounts for 83% of the metal in the precipitate, consistent with but a bit lower than that found by elemental analysis of the solid (Table 6)

Table 6. Initial and final concentration of cations in solution from magnesium hydroxide precipitation experiments and mass fraction of cations in the $Mg(OH)_2$ precipitates determined by ICP-OES.

		Concentration in Filtrate (mg/L)			Mass Fraction in Precipitate (%)		
Solution	Avg. pH	Na^+	Ca^{2+}	Mg^{2+}	Na^+	Ca^{2+}	Mg^{2+}
Low TDS Solution							
Initial Concentration		417	630	202			
	10.6	441	597	169	6	73	19
	11.7	803	445	0	2	26	72
	12.6	1,270	411	0	9	39	55
Medium TDS Soln.							
Initial Concentration		2,360	647	579			
	10.5	3,050	543	118	1	10	89
	11.7	3,550	576	95	5	8	87
	12.5	3,910	489	14	1	8	91
High TDS Soln.							
Initial Concentration		6,040	3,764	2,490			
	10.5	9,690	3,016	379	0	4	95
	11.6	11,040	3,169	5	1	5	94
	12.5	12,700	1,208	0	1	32	67

The solids produced by high pH magnesium hydroxide precipitation consisted of small dispersed particles as can be seen in the SEM image for precipitates from the medium TDS solution at pH 11.7 (Fig. 5). These solids settled poorly. A discussion of membrane filtration experiments to remove magnesium hydroxide solids is presented in Section 4.3.

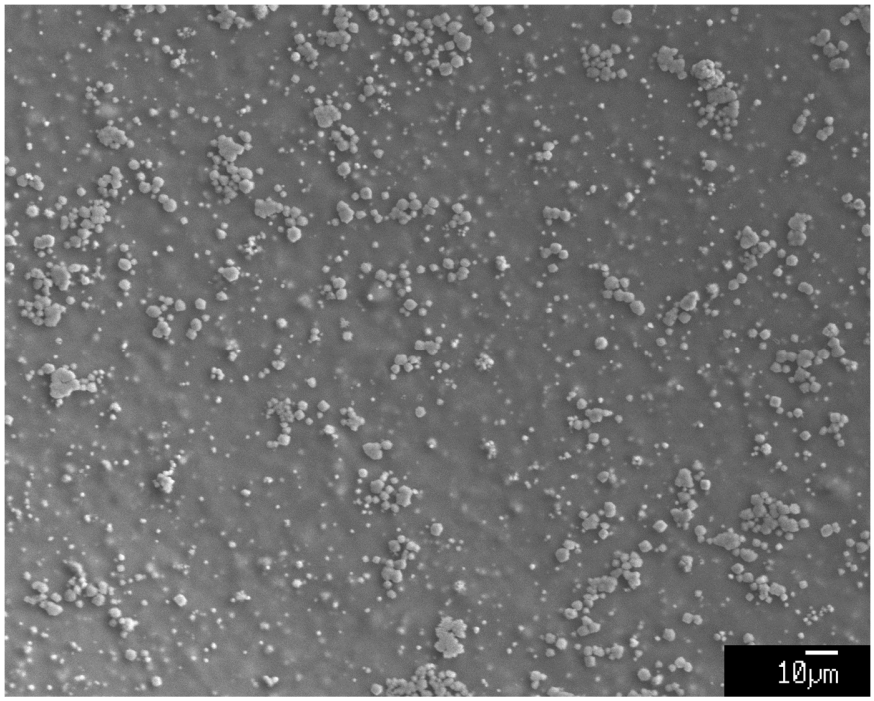

Fig. 5. SEM image of the magnesium hydroxide ($Mg(OH)_2$) precipitate from the medium TDS solution at pH 11.7.

An insufficient amount of magnesium hydroxide precipitate was collected from the low TDS solution for XRD analysis due to the low initial magnesium concentration and the small volume of solution used in the experiments. XRD analyses of solid samples precipitated from the medium TDS and high TDS solutions near pH 11.5 found that greater than 93% of the solids consisted of the mineral brucite (magnesium hydroxide) and 5% or less was calcite ($CaCO_3$). Traces of aragonite ($CaCO_3$) and portlandite ($Ca(OH)_2$) were found in some of the analyses. The purity of the magnesium hydroxide precipitate of the solids was similar at pH~11.5 and pH~12.5 but dropped to around 90% near pH 10.5.

Analyses of the solids by three methods, acid digestion, SEM-EDS, and XRD, confirm that following removal of dissolved CO_2, high pH precipitation achieves nearly complete removal of magnesium from solution and produces a high purity magnesium hydroxide precipitate.

Magnesium hydroxide precipitation kinetics has been a topic of investigation for over 50 years. Much of this research has focused on improving the kinetics of the precipitation reaction and the physical characteristics of the precipitates (Dabir et al., 1982; Brakalov, 1985; Turek and Gnot, 1995)). A more recent study that includes a comprehensive theoretical discussion of mechanism and rate of magnesium hydroxide growth has been published by Yuan et al. (2015). One method of improving the precipitation rate and particle size might be to recycle a portion of precipitate as shown in Fig. 1. This is an area that would benefit from additional research.

4.2 Gypsum Precipitation

The gypsum precipitation experiments were conducted by combining simulated regenerant from the cation exchange process with simulated concentrate from NF. The purpose of these experiments was to determine the amount of gypsum precipitated, its purity, and the residual composition of supernatant following precipitation. Note that magnesium was not included in any of these experiments as it would be removed in the first step of the MRED process. Because IX was not effective at high I (see Section 4.4), no gypsum precipitation experiments were run with simulated IX regenerant and NF concentrate from the high TDS solutions.

Table 7 lists the initial and final concentrations of major ions in the gypsum precipitation experiments which consisted of combining the NaCl brine from the IX regenerant and the concentrate from the NF process. Precipitation from an equal volume mixture of IX regenerant and NF concentrate treating low TDS water found a nearly identical drop in the molar concentrations of calcium and sulfate, which is consistent with the stoichiometry of gypsum. A similar experiment with medium TDS water found about 30% greater removal of sulfate than calcium. It is speculated that this may be due to analytical error associated with measuring dissolved constituents in very high I brines. As mentioned previously, magnesium was added to the IX regenerant from the medium TDS solution. It was not removed by gypsum precipitation and did not appear to have any effect on the precipitation process.

562 Table 7. Average measured constituent concentrations and calculated removals by gypsum precipitation from Low TDS and Medium
563 TDS solutions. All concentrations are in units of mM

	Low TDS Solution (mM)				Medium TDS Solution (mM)			
Constituent	Initial Conc.	Final Conc.	□Conc.	% Removal	Initial Conc.	Final Conc.	□Conc.	% Removal
Na^+	709.	700.	9.6	1.3	1,160.	1,211.	-48.4	-4.2
Ca^{2+}	192.5	130.9	61.7	32.0	106.4	21.4	85.0	79.9
Mg^{2+}	0.0	0.0	0.0	0.0	40.7	38.9	1.7	4.3
Cl^-	1,100.	992.	106.	9.7	1,310.	1170.	141.	10.8
SO_4^{2-}	80.1	20.2	59.9	74.8	234.3	123.8	110.5	47.2
Alkalinity *	2.7	N/M			2.2	N/M		
Predicted Removal[&]							104.	

564 * Alkalinity in units of mg/L $CaCO_3$. It was not measured (N/M) after precipitation.

565 [&] Predicted removal is the amount of gypsum calculated to precipitate from solution by PHREEQC at chemical equilibrium.

566

The two initial solutions listed in Table 7 were analyzed by a geochemical model (PHREEQC, Parkhurst and Appelo, 2013) to determine the amount of gypsum that would theoretically precipitate from each assuming chemical equilibrium conditions were reached. 73.0 mM of gypsum were precipitated from the low TDS experiments and 103.6 mM from the medium TDS experiments. The predicted molar amounts of gypsum precipitated in both solutions were close to the actual change in calcium and sulfate concentrations that were measured. No other supersaturated phases were predicted by the model. This suggests that the gypsum precipitates would be of high purity and not contain other constituents. Confirmation of this prediction is discussed below.

The precipitated gypsum was collected on membrane filters, dissolved, and the solution analyzed for major ions. Greater than 95% of the cations in the gypsum precipitate was calcium while the remainder consisted of sodium which likely came from residual water on the filtered solids.

SEM images of the precipitates from the gypsum precipitation experiments revealed well formed crystals of gypsum (Fig. 6). Other SEM images are presented in Tandukar, 2019. Elemental analysis by SEM-EDS demonstrated that the mole fractions of calcium, sulfur and oxygen were close to those for pure gypsum. XRD analyses of precipitates from the low and medium TDS gypsum precipitation experiments found that 97% and 95% of the solids were gypsum in the low TDS and medium TDS samples.

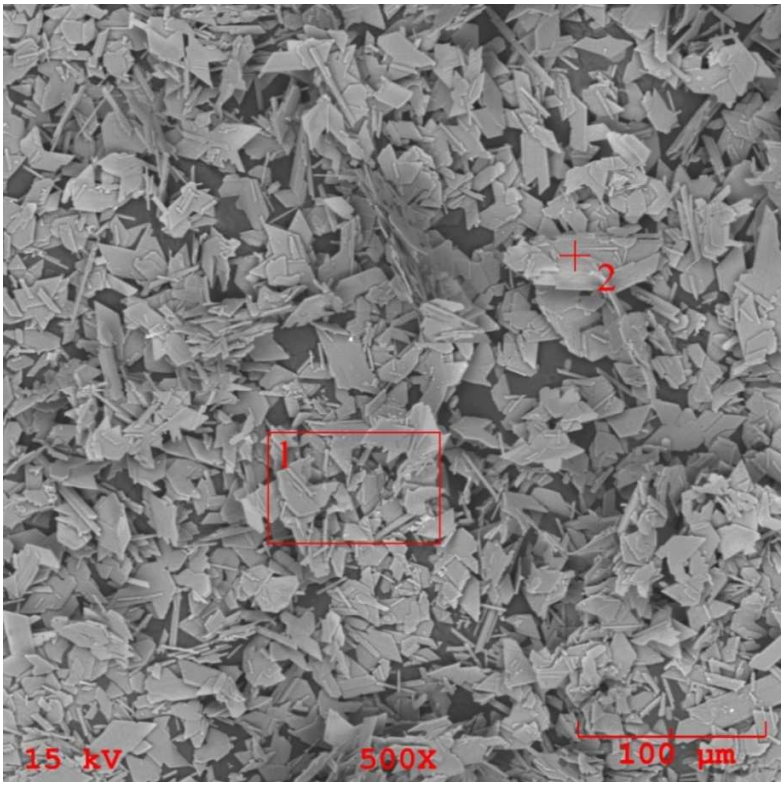

Fig. 6. SEM image at 500x for obtained gypsum sample, low TDS solution.

In contrast to magnesium hydroxide precipitates, gypsum solids settled rapidly from solution so that within 5 minutes almost all the solids had settled from a 0.5 m column. The settling velocity was found to be 106 m/d and 107 m/d for gypsum precipitates from low TDS and medium TDS solutions. This value is higher than the overflow rate for a typical clarifier of 30-60 m/d (Howe et al., 2012) suggesting that simple gravity sedimentation is appropriate for removing gypsum solids.

4.3 Membrane Filtration

Batch settling experiments were carried out for the magnesium hydroxide and gypsum precipitates. Solids from the magnesium hydroxide precipitation experiments settled poorly which was attributed to the small size of the precipitated particles (Fig. 5). The initial settling velocities of the solids were 17.3 m/d, 1.2 m/d, and 1.2 m/d from the low, medium, and high TDS solutions respectively. These settling velocities are much lower than the typical overflow

604 rates in a clarifier of 30-60 m/d (Howe, et al. 2012) and suggest that gravity settling would not be
605 an effective method for removing this precipitate.
606
607 Membrane filtration (MF) experiments were conducted to determine whether membrane
608 filtration could achieve high removal of magnesium hydroxide solids without severe and
609 irreversible fouling in a tubular membrane filter. Ninety-minute filter runs were performed
610 followed by a backwash with clean tap water. The pressure in the MF experiments remained
611 constant at 0.2 bar (3 psi) and 0.3 bar (4 psi) for slurries from the low TDS and medium TDS
612 systems respectively. The average initial turbidity of the solutions were 575 NTU and 601 NTU
613 while the average TSS concentrations were 600 mg/L and 1,270 mg/L respectively. Experiments
614 with precipitates from both low and medium TDS solutions showed a decrease in specific flux
615 with time due to increasing solids concentration in the feed tank as solids were retained in the
616 system while filtered water passed through the membrane (Fig. 7). The TSS concentration of the
617 permeate remained below 2 mg/L throughout each run which achieved greater than 99% removal
618 from both solutions. The initial turbidity of the permeate ranged between 0.4 and 0.8 NTU but
619 dropped to less than 0.3 NTU within 10 minutes of the start of the run.
620
621 A tap water backwash restored the initial flux between runs to values near that of the new
622 membrane, although the initial flux in the third run was lower than the other runs. As the third
623 run progressed the specific flux approached that for the other runs which indicated that the
624 membrane was not irreversibly fouled.
625
626 Following completion of the third run from the low TDS solution, the system was cleaned by
627 circulating 1% citric acid through the feed side of the system for one hour and recycling both the
628 feed solution and the filtrate back to the feed tank. The permeate flow of citric acid through the
629 membrane during cleaning was not measured. After cleaning the system was rinsed with tap
630 water.

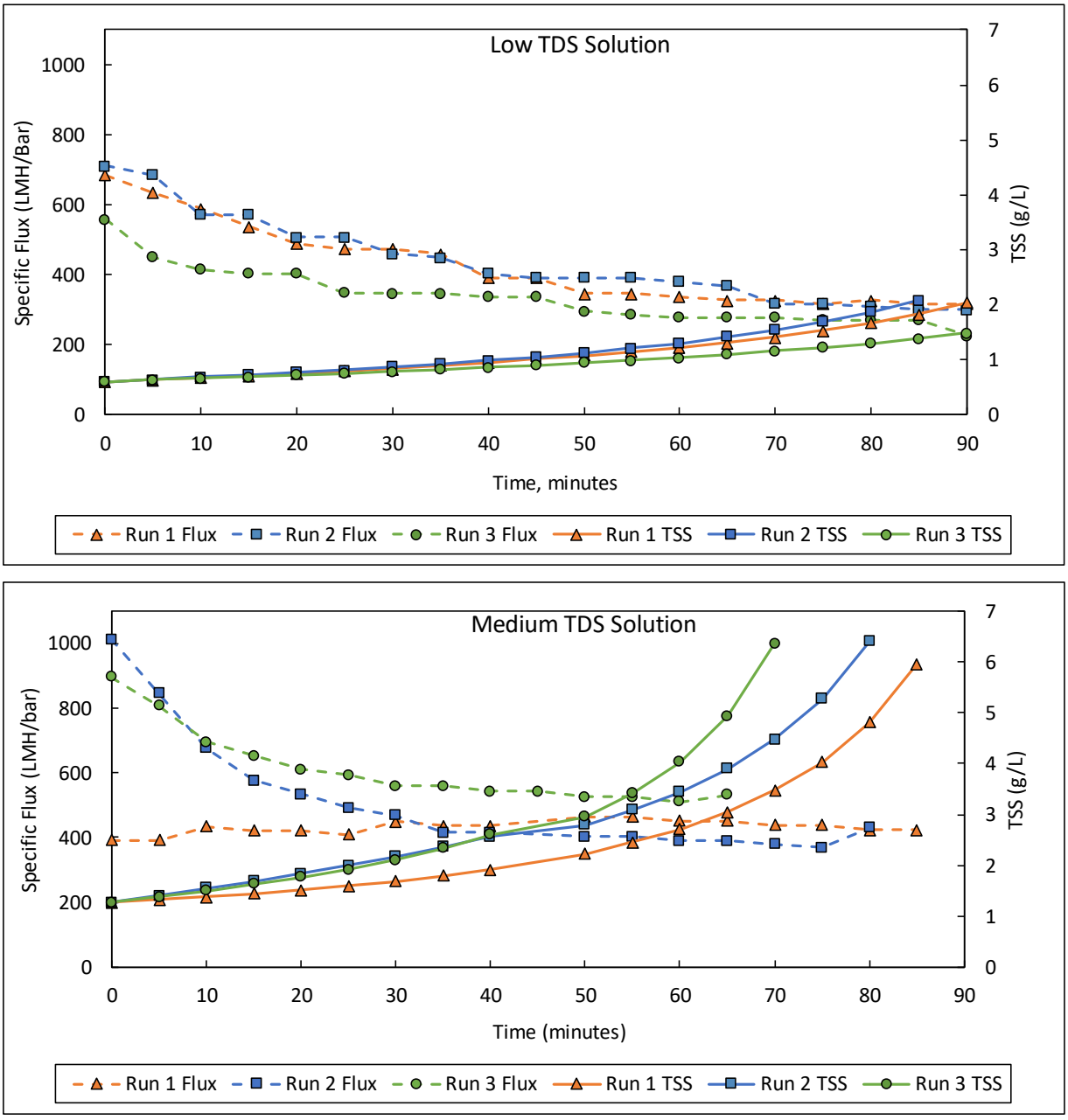

Fig. 7. Specific permeate flux and feed tank TSS as a function of run time for three runs at low TDS solutions (top) and medium TDS solutions (bottom).

A series of experiments were run in which both the retentate and filtrate were recycled. The results showed no decrease in specific flux over the 90 minute filter runs. The specific fluxes were 250 LMH/bar and 640 LMH/bar for magnesium hydroxide filtration from the low TDS and medium TDS solutions respectively. Note the low initial flux for Run number 1 for the medium

TDS solution (Fig. 7). This run was done following a citric acid cleaning after which the membrane was inadvertently not backwashed with tap water which may have left some solids on the membrane. Subsequent tap water backwashes after runs 1 and 2 restored the initial flux of the membrane as shown in the figure confirming the ability to clean the membrane. The results of the filtration experiments and the tap water and citric acid cleaning experiment suggest that membrane filtration is an effective method for removing fine magnesium hydroxide particles.

4.4 Batch IX Experiments to Determine Resin Selectivity

Batch IX experiments were conducted to determine the effect of ionic strength on resin selectivity. The binary separation factor ($\alpha_{Ca/Na}$) was determined by fitting exchange isotherms for binary solutions of Na^+ and calcium for solutions at I values ranging from 0.01 M to 1 M. The graphs for calcium and sodium cation exchange for SSTC60 resin are presented in Fig. 8 for the SSTC60 resin. Similar results were found for the Amberlite HPR 1300 resin and are reported by Shahi (2019). The binary separation factor $\alpha_{Ca/Na}$ ranged from 5.5 at I = 0.01 M to 0.65 at I = 1 M. A binary separation factor of less than 1 means that the resins were more selective for sodium than for calcium and will not selectively remove calcium from solution. This is due to the effects that I has on the divalent/monovalent separation factor which tends to reverse in favor of the monovalent ion at high I (Clifford et al., 2011).

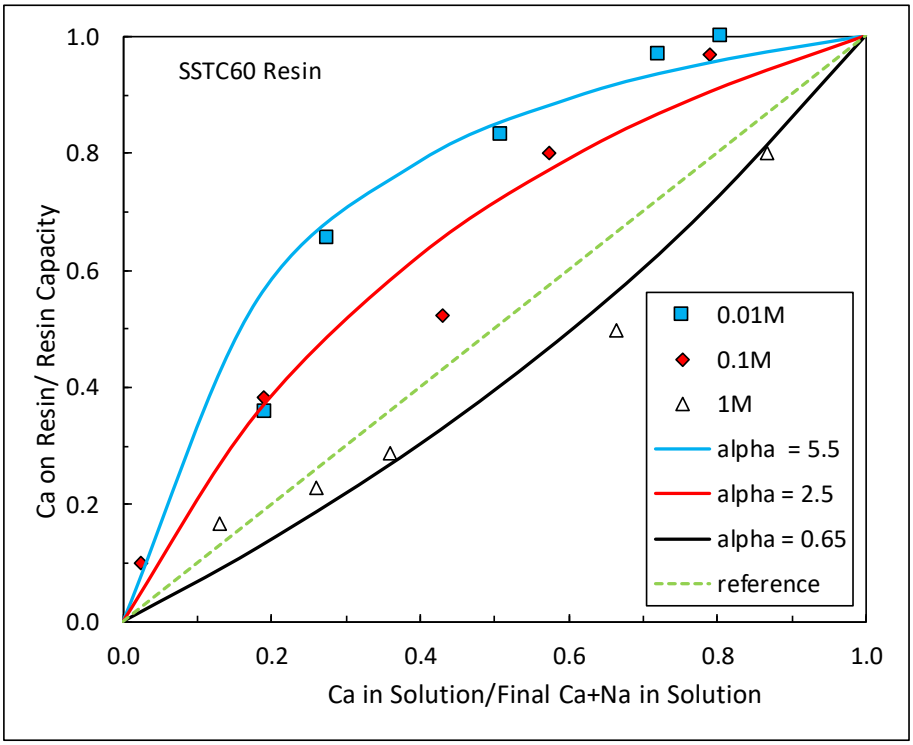

Fig. 8. Ion exchange electroselectivity for calcium as a function of ionic strength for divalent-monovalent (Ca^{2+}/Na^{+}) cation exchange for SSTC60 Resin.

4.5 Cation Exchange Column Experiments

In an IX column, breakthrough occurs when the effluent calcium concentration reaches 10% of its initial concentration and exhaustion is reached when the effluent concentration reaches 90% of the initial concentration. A series of experiments in which the columns were run to exhaustion and regenerated with four BVs of 10% NaCl showed that the resins could be completely regenerated, and found no evidence of irreversible sorption (see Howe et al., 2020; Shahi, 2019).

Column experiments were run to measure breakthrough curves of the IX resins for waters of varying TDS. Duplicate columns were run for each experiment. For high TDS water, the calcium breakthrough was reached at 1 BV and exhaustion was reached at 6 BVs (Fig. 9), which is consistent with low resin preference for calcium. Medium TDS brackish water reached exhaustion at 12 BVs, while low TDS brackish water did not reach exhaustion until after 65 BVs. The volume of water treated prior to reaching exhaustion ($C/C_o = 0.9$) is summarized in Table 8. The small number of BVs of high TDS water treated before reaching column

exhaustion is consistent with the low value of the binary separation factor, $\alpha_{Ca/Na}$ as I increases from 0.01 M to 1 M (see Figure 8)

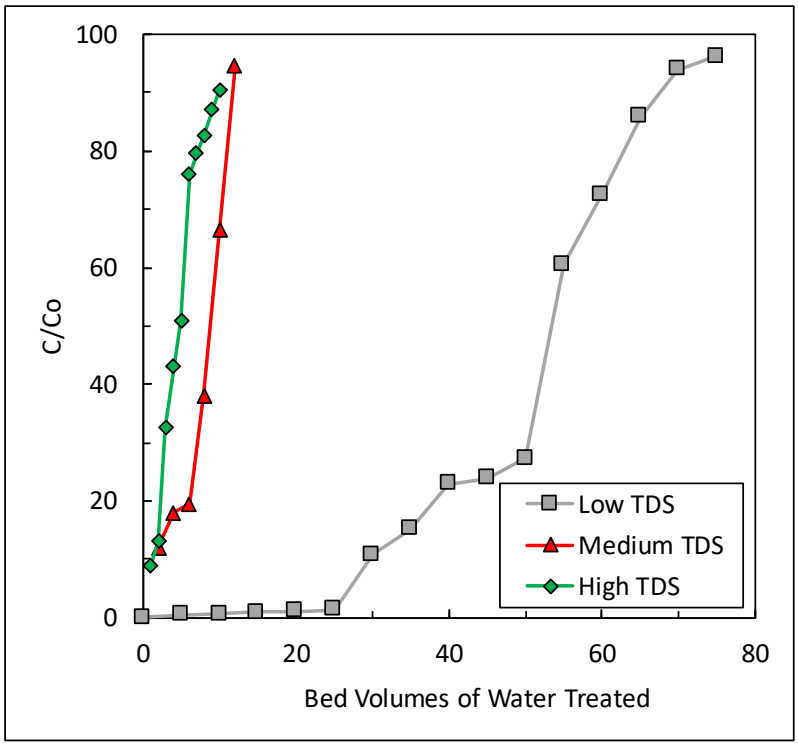

Fig. 9. Breakthrough Curve for calcium removal by IX for low, medium, and high TDS water using SSTC60 resin. Values shown are average of duplicate experiments.

Table 8. Number of bed volumes of water treated prior to reaching exhaustion of the IX column ($C/C_o = 0.9$).

Solution	TDS (mg/L)	Ionic Strength (M)	No. of BVs to Exhaustion
Low TDS Soln.	5,900.	0.19	65
Medium TDS Soln.	28,800.	0.63	12
High TDS Soln.	52,600.	1.03	6

Regeneration experiments were carried out to determine the best procedure for regenerating the IX columns to provide a high Ca^{2+} concentration in the regenerant. Flow rates of 10% NaCl

regenerant solutions were used ranging from 2.5 mL/min to 10 mL/min corresponding to empty bed contact times (EBCT) ranging from 30 to 7 minutes. The results demonstrate that slower flow rates required less total volume to achieve column regeneration with the lowest regenerant volume produced at a flow rate of 2.5 mL/min.

Based on the results of the batch and column IX experiments, an approximate I of 0.2 M was estimated to be the highest concentration where IX can be used for selective removal of calcium. The actual upper limit will depend on the solution composition in addition to I. The ability of the IX process to separate calcium from monovalent ions at high I establishes the upper limit for the MRED process. Depending on the ions present in solution, this corresponds to a TDS concentration of approximately 10,000 mg/L.

4.6 Nanofiltration Modelling and Experimental Results

Water Application Value Engine (WAVE) software developed by Dow Water & Process Solutions was used to simulate nanofiltration using Dow Filmtec NF270-400-34i nanofiltration membranes. A three stage NF system was modeled for the low TDS solution and a four stage NF system was modeled for the medium TDS solution. This number of stages will achieve 90% feed water recovery. Modeling was only done for the low and medium TDS solutions because the IX process was not effective for high TDS solution.

The model predicted about 95% sulfate rejection from both low and medium TDS solutions, while chloride rejection was about 20%. Sodium rejection was predicted to be approximately 55%. The high rejection of monovalent sodium compared to chloride is caused by the need to maintain electroneutrality in the NF permeate and concentrate; since NF concentrate has a high concentration of anionic sulfate, cationic sodium must also be retained.

Experiments were conducted using a 160 cm^2 flat sample of the NF270 membrane in a custom designed pressure system for low and medium TDS solutions at three feed pressures. Sulfate rejections of 94% and 91 % were measured for the low and medium TDS waters. Sodium rejection was measured at 61% at low TDS and 49 % for the medium TDS solution. Chloride rejection was less than 20% for both low and medium TDS solutions. The experimental results

are consistent with those predicted by the WAVE model. The results demonstrate the ability of NF to achieve high sulfate removal that, when combined with calcium removal in the IX column, will produce a product water that has very low scale forming potential in a subsequent desalination process.

4.7 Discussion of Experimental Results

The experimental program investigated three principal unit operations of the MRED process for treating hard brackish and saline waters. The objectives were to: (1) demonstrate that high purity magnesium hydroxide could be precipitated at high pH after removal of dissolved carbon dioxide; (2) that IX could selectively remove calcium from high I waters; (3) that NF could selectively concentrate sulfate; and (4) that IX regenerant containing calcium and NF concentrate containing sulfate could be combined to precipitate high purity gypsum. These objectives were achieved in experiments using simulated wastewater from the flue gas desulfurization (FGD) process.

However, FGD wastewater represents only one of many different possible brackish or saline water characteristics that might be amenable to treatment by the MRED process. Three classes of compounds that are often found in brackish water that were not studied experimentally include: (1) iron, manganese, strontium and other metals; (2) silica, and (3) dissolved organic matter (DOM). The expected removal of these constituents by the MRED process is briefly discussed here.

Oxidized forms of iron, manganese, and many other transition metals form insoluble oxide or hydroxide phases at high pH (Stumm and Morgan, 1996; Langmuir, 1997; Benjamin, 2015). The first step in the MRED process, air stripping to remove dissolved carbon dioxide, will establish oxidizing conditions in the solution. Raising the pH to greater than 11 will then result in precipitation of iron and manganese (Crittenden et al., 2012) as well as copper, lead, mercury, nickel, zinc and other metals (Fu and Wang, 2011). High pH precipitation of magnesium hydroxide will also remove dissolved silica (SiO_2) (Randtke, 2011; Turek and Gnot, 1995). Removal of these constituents will decrease the purity of the magnesium hydroxide, however, except in the most unusual circumstances the molar concentration of magnesium in hard water is

orders of magnitude greater than the concentration of other metals or silica so the impact on the quality of the magnesium hydroxide precipitate will be small.

Strontium and barium, if present, would not be removed by high pH precipitation because they do not form insoluble hydroxides. They would, however, be removed by IX and subsequent gypsum precipitation. Their sulfate phases, $SrSO_4$ and $BaSO_4$, are less soluble than gypsum. As with metals removed by high pH precipitation, high concentrations of these strontium or barium would affect the purity of the gypsum precipitate, however a water with this chemistry would be most unusual.

Dissolved organic matter (DOM), if present at high concentrations, might present a challenge to the MRED process. It would not be removed by high pH precipitation or cation exchange, though its removal by anion exchange is well known (Levchuk et al., 2018; Bolto et al., 2004). Dissolved organic matter is effectively removed by NF, which would protect a subsequent desalination process, however, at high concentrations it can lead to membrane fouling (Siddiqui et al., 2000). There is a large body of literature on membrane fouling by DOM that cannot be discussed here, however, reviews of the topic have been published by Contreras et al., (2009) and Al-Amoudi (2010).

Different chemical composition of brackish and saline waters may affect the performance of one or more of the unit operations in the MRED process. However, each of these unit operations are well understood and widely used in water and wastewater treatment. Nevertheless, because of the unusual sequence of operations and unique objectives of the MRED process, it is suggested that conducting simple laboratory experiments such as those described in this paper may be appropriate to confirm process performance prior to designing a prototype system for full-scale application. Such testing would be especially important if the feed water had high concentrations of metals other than alkali or alkaline earth metals (i.e. sodium, potassium, calcium and magnesium) or high concentrations of DOM.

5 Process Flow Model

The MRED process is based on conventional water treatment unit operations that are well understood, however, they are applied in a unique sequence with high I feed water to achieve uncommon objectives. To understand and optimize the overall process a mass and chemical balance model was developed to predict mass and volumetric flows of water and major ions in solution.

The process flow model calculates flows and solution chemistry following each unit operation in the MRED process at the numbered locations shown in Fig. 1. The model was constructed in Microsoft Excel as a series of linked worksheets. The model determines flows and chemistry for the magnesium hydroxide and gypsum slurries, the concentrate from the NF process, and the IX regenerant flow, as well as the chemistry of the supernatant from the gypsum precipitation process.

To demonstrate the model's capabilities and the overall performance of the MRED process, the flows and chemistry to treat 1,900 m^3/d (500,000 gal/d) of the low TDS (4,290 mg/L) water with the composition shown in Table 1 are summarized. The chemistry at each step is presented in units of milliequivalents per liter (meq/L) which is appropriate for calculations involving acid-base, precipitation, and ion exchange reactions. The solution chemistry after each process is displayed as pairs of horizontal bar graphs in which the top bar represents the concentration of major cations in the solution and the lower bar shows the major anions (Fig. 10).

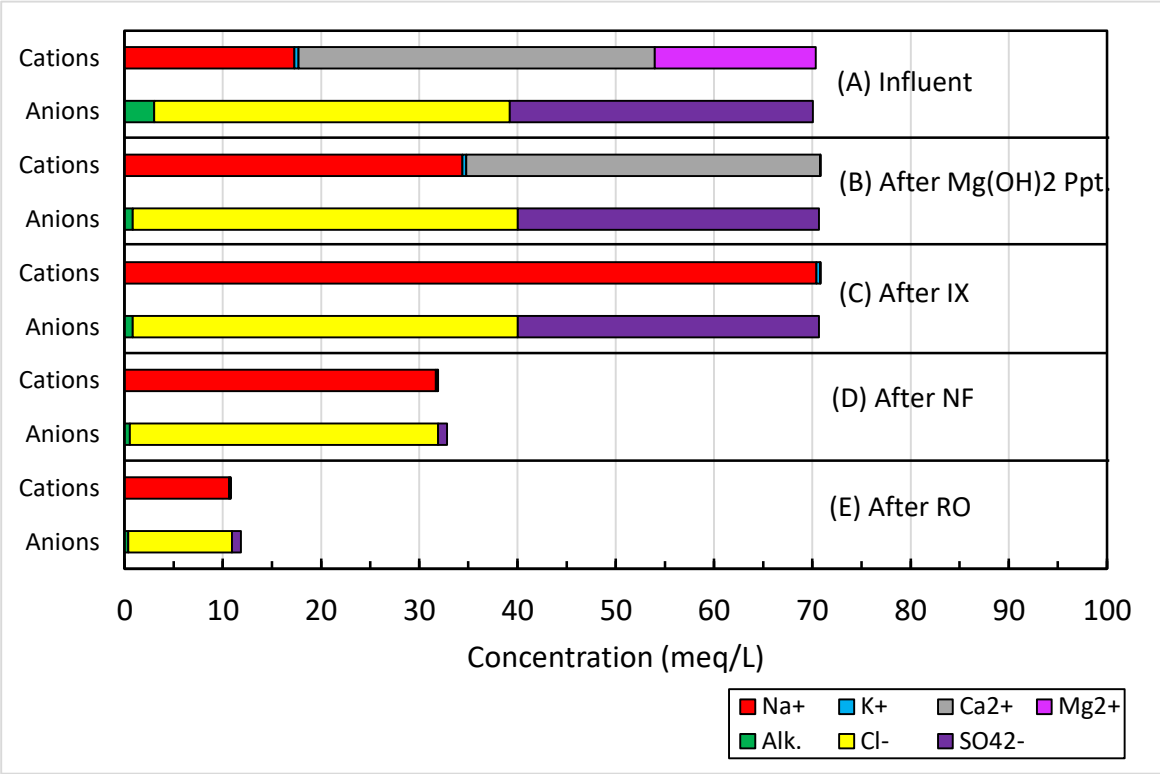

Fig. 10. Summary of water chemistry after each major unit operation in the MRED process.

The first steps in the MRED process involve acid addition, to lower the pH to less than 4.5, air stripping, to remove dissolved CO_2, and raising the pH to 11.5, to precipitate magnesium hydroxide. Addition of acid destroys the alkalinity (the buffer capacity) and degasification removes CO_2, which reduces the amount of base (NaOH) needed to raise the pH to precipitate magnesium hydroxide. The amount of base required is determined by the stoichiometry of the magnesium hydroxide precipitation reaction plus an additional amount to raise the pH to 11.5 that is determined by calculating the alkalinity of the final solution. In the example scenario, magnesium hydroxide precipitation generates 906 kg/d of solids at a flow rate of 43 m^3/d assuming a 0.6% solids concentration from the MF process based on performance of MF systems treating drinking water (AWWA, 2003).

The cations in the water entering the IX process consist of only sodium at 34 meq/L and calcium at 36 meq/L (Fig. 10B). It is assumed that the IX operation will remove all of the calcium. The BVs of water that can be treated by the IX process is determined by the calcium concentration in

819 the feed water and the IX resin capacity. After removing magnesium hydroxide and calcium, the
820 water entering the NF process contains no calcium or magnesium so that the major ions consist
821 only of sodium, chloride and sulfate Fig. 10C).
822
823 Experimental data and WAVE modeling suggest that the NF process will remove 96% of the
824 sulfate, ~20% of chloride, and ~55% of sodium. Using these values produces the chemistry of
825 the NF permeate shown in Fig. 10D. The NF concentrate consists almost entirely of sodium and
826 chloride which enables subsequent desalination with little fouling potential. Fig. 10D
827 demonstrates that the NF process partly desalinates the solution and reduces the total
828 concentration of ions from 140 meq/L to about 60 meq/L.
829
830 The IX regenerant chemistry has a high calcium concentration, while the NF concentrate has a
831 high sulfate concentration. The sulfate concentration in the NF concentrate is about 300 meq/L
832 whereas the calcium concentration in the IX regenerant is 900 meq/L, three times higher.
833 However, the flow of NF concentrate (discussed below) is almost exactly three times that of the
834 IX regenerant so a stoichiometric balance of calcium and sulfate is maintained.
835
836 The desalination concentrate is used to regenerate the IX columns; after regeneration it is
837 combined with high sulfate concentrate from the NF process to precipitate gypsum. As
838 demonstrated in this research, gypsum settles well and can be removed by gravity settling. 3,900
839 kg/d of gypsum will precipitate as a 50 m^3/d slurry using a 7% settled solids concentration found
840 by Tandukar (2019). Note, however, that gypsum is a relatively soluble mineral. Results
841 summarized in Table 7 show that the final calcium and sulfate concentrations after gypsum
842 precipitation when treating the low TDS water are 130 mM and 20.2 mM respectively. This
843 supernatant from gypsum precipitation can be returned to the IX process to recover the
844 remaining calcium and sulfate as shown in Fig. 1.
845
846 The final step in the MRED process is desalination. It can be a membrane process such as RO or
847 a thermal process such as distillation, membrane distillation or other method. Regardless of the
848 method used, the water fed to the desalination process will have lower TDS and negligible
849 fouling potential due to removal of calcium, magnesium, sulfate, dissolved CO_2 and silica.

Desalination by RO was modeled assuming 98% feed water recovery based on a 60 meq/L (1,750 mg/L) NaCl feed water with negligible fouling potential. For this water chemistry a seawater desalination system would be appropriate. RO ion rejection values from the WAVE model were used in the process model. The final treated and desalinated water is projected to have a final TDS concentration of less than 600 mg/L (Fig. 10E). The concentrate from the RO process has an ionic strength of 1.1 M and a TDS of approximately 62,000 mg/L (Fig. 11). This solution, consisting almost entirely of sodium and chloride ions, is used to regenerate the IX columns. Note that the 6.2% salt concentration of the RO concentrate is less than the 10% solution used in the experimental program. The lower concentration means that a greater volume of concentrate will be recycled to regenerate the IX columns, approximately 5 BVs instead of 4 BVs.

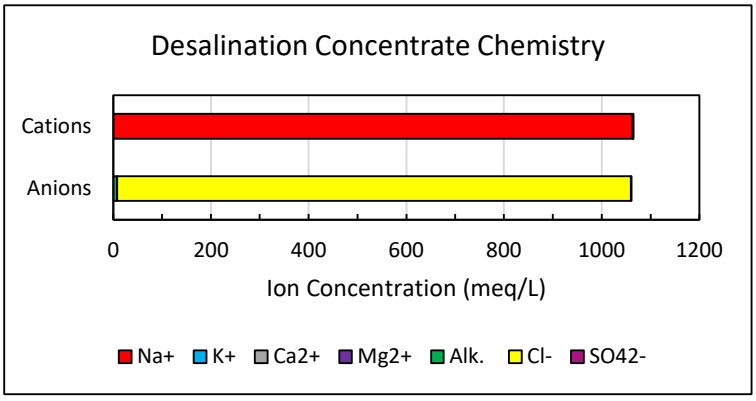

Fig. 11. Water chemistry of the RO concentrate stream.

At each step in the MRED process the flows of water into and out of each unit operation, and the volumetric flows of slurries produced by the operation are summarized in Table 9. The example described in this section was modeled to treat a low TDS FGD wastewater with the chemistry shown in Table 1. For an influent flow of 1,900 m^3/d the MRED process recovers 1,560 m^3/d of high quality desalinated water for a feed water recovery of 82%. Furthermore, by recycling the supernatant from the gypsum precipitation process, an additional 175 m^3/d of water may be retained for an overall feed water recovery of 91%. This reduces the concentrate stream by

873 approximately 58%, which greatly reduces the volume of water that must be disposed of. A
874 summary of the overall process performance is presented in Table 9.
875
876 Note that the influent concentrations of calcium and sulfate expressed as meq/L were
877 approximately the same for the water modeled here (see Table 1) because it was based on FGD
878 wastewater. Unless there was a large imbalance, it would be feasible to produce approximately
879 equal concentrations of calcium and sulfate through addition of an alternative acid or base. For
880 example, substitution of sulfuric acid (H_2SO_4) for hydrochloric acid would increase the
881 concentration of sulfate ions while addition of hydrated lime ($Ca(OH)_2$) instead of caustic soda
882 (NaOH) would increase the calcium concentration. Both sulfuric acid and lime are less
883 expensive chemicals than hydrochloric acid and caustic soda which would reduce the treatment
884 costs.
885 Table 9. Summary of volumetric and mass flows for treating 1,900 m^3/d of brackish
886 groundwater.

Parameter	Units	Value
Influent flow	m^3/d	1,900.
Mass of $Mg(OH)_2$ recovered	kg/d	906.
Vol. of $Mg(OH)_2$ recovered	m^3/d	143.
Mass of gypsum recovered	kg/d	3,850.
Vol. of gypsum recovered	m^3/d	50.
Treated water flow	m^3/d	1,740.
Fractional feed water recovery	%	91.

887

888 Conclusions

889 This paper describes the Mineral Recovery and Enhance Desalination (MRED) process to
890 recover commodity minerals from brackish water, which will in turn facilitate recovery of a large
891 fraction of the feed water by a conventional desalination process. The process uses conventional
892 water treatment processes that are well understood and widely used, but they are applied in a
893 unique sequence to achieve innovative objectives. After desalination, the treated water will be of

high quality and suitable for public supply or other applications. Equally important, the process developed in this project greatly reduces the volume and mass of waste associated with brackish water desalination which will result in significant waste disposal cost savings.

Experimental results showed that high purity magnesium hydroxide was produced by precipitation at pH 11.5 or greater, and this process removed nearly 100% of the dissolved magnesium . However, the process produced solids that settled poorly. Subsequent experiments demonstrated that these solids could be effectively removed by membrane filtration with low fouling of the membrane.

Batch and column experiments conducted with cationic IX resins confirmed that resin selectivity for divalent calcium ions decreases markedly as the ionic strength increased above about 0.2 mol/L. Decreasing IX performance at high ionic strength establishes the maximum salinity for waters that can be treated by the MRED process. The high NaCl brine in a desalination concentrate can be used to regenerate the IX resin, thus eliminating the need to purchase salt for the process.

Nanofiltration (NF) after removal of magnesium and calcium will selectively remove sulfate from solution. Greater than 95% sulfate removal and about 20% chloride removal was demonstrated. The high sulfate concentrate stream from the NF is combined with the high calcium IX regenerant brine to precipitate gypsum.

Gypsum precipitation experiments showed that calcium can be recovered from hard brackish water at greater than 95% purity by mixing IX regenerant and the NF concentrate. The gypsum solids settled well and can be removed from solution by gravity settling.

A steady state mass balance model was developed for the MRED process which calculates the volumes of all flows in the process, including those associated with chemical addition. It also calculates the masses and volumetric flows of the slurries of magnesium hydroxide and gypsum generated by the treatment operations. An example calculating using this model it predicted that a 1,900 m^3/d flow of brackish water would recover 906 kg/d of magnesium hydroxide, 3,850

kg/d of gypsum, and 91% of the feed water would be recovered as high quality desalinated water.

A wide variety of water chemistries of hard brackish or saline water are possible depending \ on the source of the water. For example, brackish groundwater from a karst formation will be different from wastewater from an industrial process. The results presented here were based on FGD wastewater chemistry which will be different than either of these. The results presented here suggest that MRED process will effectively achieve the goals of recovering commodity minerals, reducing waste management and disposal costs, and improving feed water recovery by a subsequent desalination process. The effectiveness of the process for treating other waters will vary depending on its chemistry.

References

Al-Amoudi, A.S. Factors Affecting Natural Organic Matter (NOM) and Scaling Fouling in NF Membranes: A Review. Desalination 259, (2010) 1–10. https://doi.org/doi.org/10.1016/j.desal.2010.04.003

Allam, A.R., E.-J. Saaf, M.A. Dawoud. Desalination of Brackish Groundwater in Egypt. *Desalination* 152(1–3), . (2003), 19–26. https://doi.org/10.1016/S0011-9164(02)01044-5.

Altaf, M.A., D. Whittington, H. Jamal, and V.K. Smith.. Rethinking Rural Water Supply Policy in the Punjab, Pakistan *Water Resources Research* 29(7), (1993), 1943–54. https://doi.org/10.1029/92WR02848.

Anis, S.F., R. Hashaikeh,, N. Hilal. Reverse osmosis pretreatment technologies and future trends: A comprehensive review. Desalination 452, (2019), 149–195. https://doi.org/doi.org/10.1016/j.desal.2018.11.006

APHA, AWWA, & WEF.. *Standard methods for the examination of water and wastewater*, 23rd ed. American Public Health Association, American Water Works Association, Water Environment Federation, Washington, D.C. (2017) ISBN 9780875532875.

AWWA, AWWA Residuals Management Research Committee. Committee Report: Residuals Management for Low-Pressure Membranes. *J. Am. Water Works Assoc.* 9 (6), (2003), 68–82.

Ben Ahmed, S., M.M. Tlili, M. Amami, M. Ben Amor, M.. Gypsum Precipitation Kinetics and Solubility in the NaCl–MgCl2 –CaSO4 –H2O System. *Industrial & Engineering Chemistry Research*, *53*(23), (2014), 9554–9560. doi.org/10.1021/ie5004224

Benjamin, M. M. Water chemistry. 2nd ed. McGraw-Hill Education: New York, NY, (2015), 907 p., ISBN 978-1478623083

Bolto, B., D. Dixon, R. Eldridge. Ion Exchange for the Removal of Natural Organic Matter. Reactive and Functional Polymers 60, (2004), 171–182. https://doi.org/doi.org/10.1016/j.reactfunctpolym.2004.02.021

Brakalov, L.B. On the Mechanism of magnesium hydroxide tipening. Chemical Engineering Science 40, (1985), 305–312. https://doi.org/doi.org/10.1016/0009-2509(85)80071-3

Buono, R.M., K.R. Zodrow, P.J.J. Alvarez, Q. Li. Brackish Groundwater: Current Status and Potential Benefits for Water Management. Issue Brief. Houston, TX: Rice University's Baker Institute for Public Policy. (2016) https://scholarship.rice.edu/bitstream/handle/1911/91263/BI-Brief-041116-CES_Groundwater.pdf?sequence=1.

Clifford, D., T.J. Sorg, G. Ghurye. Ion Exchange and Adsorption of Inorganic Contaminants, Ch. 12 *Water Quality and Treatment: A Handbook on Drinking Water*, McGraw-Hill, Inc., New York, (2011) ISBN 978-0-07-163011-5

Contreras, A., A. Kim, Q. Li. Combined Fouling of Nanofiltration Membranes: Mechanisms and Effect of Organic Matter. J. of Membrane Science, 327, (2009), 87–95. https://doi.org/doi.org/10.1016/j.memsci.2008.11.030

Crittenden, J.C., R.R. Trussell, D.W. Hand, K.J. Howe, G. Tchobanoglous, G.. MWH's Water Treatment Principles and Design, 3rd ed. John Wiley & Sons, Hoboken, NJ. (2012), ISBN 978-0-470-40539-0

Dabir, B., R.W. Peters, J.D. Stevens. Precipitation Kinetics of Magnesium Hydroxide in a Scaling System. Industrial & Engineering Chemical Fundamentals 21, (1982), 298–305.

Dow Water & Process Solutions. (2019). http://msdssearch.dow.com/PublishedLiteratureDOWCOM/dh_099c/0901b8038099ccfc.pdf?filepath=liquidseps/pdfs/noreg/609-50306.pdf&fromPage=GetDoc..

EPWU. Desalination, El Paso Water Utility. El Paso Water Utility. 2020. (2020) https://www.epwater.org/our_water/water_resources/desalination.

986 Farias, E.L., K.J. Howe, B.M. Thomson. “Spatial and Temporal Evolution of Organic Foulant
987 Layers on Reverse Osmosis Membranes in Wastewater Reuse Applications. *Water Research*
988 58, (2014),102–110.
989 Fu, F., Q. Wang. Removal of Heavy Metal Ions from Wastewaters: A Review. J. of
990 Environmental Management 92, (2011), 407–418.
991 https://doi.org/doi.org/10.1016/j.jenvman.2010.11.011
992 Hadadin, N., M. Qaqish, E. Akawwi, A. Bdour. Water Shortage in Jordan - Sustainable
993 Solutions. *Desalination,* 250(1), (2010), 197–202.
994 https://doi.org/10.1016/j.desal.2009.01.026.
995 Howe, K. J., D.W. Hand, J.C. Crittenden, R.R.Trussell, G. Tchobanoglous. *Principles of water*
996 *treatment*. John Wiley & Sons, Inc., (2012) ISBN 978-0470405383
997 Howe, K.J., B.M. Thomson, S. Tandukar, A.Shahi, C.O. Lee, C.O Flue Gas Desulfurization
998 Wastewater Treatment, Reuse, & Recovery, Final Report to DOE National Energy
999 Technology Laboratory, Morgantown, WV, (2020), 176 p.
1000 Jaber, J.O., M.S. Mohsen. Evaluation of Non-Conventional Water Resources Supply in Jordan.
1001 *Desalination,* 136(1–3), (2001), 83–92. https://doi.org/10.1016/S0011-9164(01)00168-0.
1002 Kalaswad, S., B. Christian, and R. Petrossian. Brackish Groundwater in Texas. In *The Future of*
1003 *Desalination in Texas, 2*, 13. Texas Water Development Board. (2005),
1004 https://www.twdb.texas.gov/publications/reports/numbered_reports/doc/R363/B2.pdf.
1005 Kosutic, K., I. Novak, L. Sipos., B. Kunst. Removal of Sulfates and other inorganics from
1006 potable water by nanofiltration membranes of characterized porosity. *Separation*
1007 *purification technology*, 37, (2004), 177-185, doi:10.1016/S1383-5866(03)00206-5
1008 Langmuir, D. *Aqueous Environmental Geochemistry.* . Upper Saddle River, NJ: Prentice Hall,
1009 (1997), 600 p., ISBN-13: 978-0023674129.
1010 Levchuk, I., J.J.R. Marquez, M. Sillanpaa, M. Removal of Natural Organic Matter (NOM) frm
1011 Water by Ion Exchange - A Review. Chemosphere 192, (2018), 90–104.
1012 https://doi.org/doi.org/10.1016/j.chemosphere.2017.10.101
1013 McMahon, P.B., J.K. Bohlke, K.G. Dahm, D.L. Parkhurst, D.W. Anning, J.S. Stanton.. Chemical
1014 Considerations for an Updated National Assessment of Brackish Groundwater Resources.
1015 *Groundwater,* 54(4), (2015), 464–75. https://doi.org/10.1111/gwat.12367.

Nashed, A., A.B. Sproul, G. Leslie. Water Resources and the Potential of Brackish Groundwater Extraction in Egypt: A Review. *J. of Water Supply: Research and Technology - Aqua,* 63(6), (2014), 399–428. https://doi.org/10.2166/aqua.2014.162.

Newton, B.T., L.L. Land. Brackish Water Assessment in the Eastern Tularosa Basin, New Mexico, Open-File Report 582. Socorro: NM Bureau of Geology & Mineral Resources. (2016). https://geoinfo.nmt.edu/publications/openfile/downloads/500-599/582/OFR-582_ETB_brackishLR.pdf.

NMBGMR. New Mexico: Regional Brackish Water Assessment, NM Bureau of Geology and Mineral Resources. (2018) https://geoinfo.nmt.edu/resources/water/projects/bwa/home.html.

Parkhurst, D.L., C.A.J. Appelo. Description of Input and Examples of PHREEQC Version 3 - A Computer Program for Speciation, Batch-Reaction, One-Dimensional Transport and Inverse Geochemical Calculation. Chapter 43 of Section A, Groundwater Book 6, Modeling Techniques. Denver, CO: U.S. Geological Survey. (2013) https://pubs.usgs.gov/tm/06/a43/pdf/tm6-A43.pdf.

Pilarska, A. A., L. Klapiszewski, T. Jesionowski. Recent development in the synthesis, modification and application of Mg(OH)2and MgO: A review. *Powder Technology*, *319*, (2017) 373–407, doi.org/10.1016/j.powtec.2017.07.009

Randtke, S.J. Precipitation, Coprecipitation, and Precipitative Softening. In *Water Quality & Treatment: A Handbook on Drinking Water, 6th Ed.*, J.K. Edzwald (Ed.), McGraw-Hill, New York, NY. (2011) ISBN 978-0-07-163011-5

Ruiz-Garcia, A., I. Nuez,, M.D. Carrascosa-Chisvert, J.J. Santana Simulations of BWRO Systems Under Different Feedwater Characteristics. Analysis of Operation Windows and Optimal Operating Points. Desalination, 491, (2020), 114582 . https://doi.org/doi.org/10.1016/j.desal.2020.114582

Ruiz-Garcia, A., J. Feo-Garcia. Estimation of maximum water recovery in RO desalination for different feedwater inorganic compositions. Desalination and Water Treatment 70, (2017), 34–45. https://doi.org/doi.org/10.5004/dwt.2017.20476

Ruiz-Garcia, A., N. Melian-Martel,, I. Nuez. Short Review on Predicting Fouling in RO Desalination. Membranes 7, 62, (2017), https://doi.org/doi.org/10.3390/membranes7040062

Sengupta, A. K.. *Ion Exchange in Environmental Processes.* Hoboken: Wiley, (2017), 496 p., ISBN: 978-1-119-15739-7

Shahi, A. R.. *Application of Ion Exchange and Nanofiltration to treat flue gas desulfurization wastewater,* M.S. Thesis, University of New Mexico, Albuquerque, NM. (2019) https://digitalrepository.unm.edu/ce_etds/230

Siddiqui, M., G. Amy, J. Ryan, W. Odem. Membranes for the Control of Natural Organic Matter from Surface Waters. Water Research 34, (2000), 3355–3370. https://doi.org/doi.org/10.1016/S0043-1354(00)00024-5

Stanton, J.S., D.W. Anning, C.J. Brown, R.G. Moore, V.L. McGuire, S.L. Qi, A.C. Harris, K.F.Dennehy, P.B. McMahon, J.R. Degnan, J.K.Bohlke. Brackish Groundwater in the United States. Professional Paper 1833. Reston, VA: U.S. Geological Survey. (2017) https://doi.org/10.3133/pp1833.

Stanton, J.S., K.F. Dennehy. Brackish Groundwater and Its Potential to Augment Freshwater Supplies. USGS Fact Sheet 2017-3054. Groundwater Resources for the Future. Reston, VA: U.S. Geological Survey. (2017) https://doi.org/10.3133/fs20173054.

Stariha, V.B., K. Dahm, K. Guerra, A. Tiffenbach. Estimating the Cost of Brackish Groundwater Desalination in Texas, Final Report Submitted to the Texas Water Development Board. Denver, CO: U.S. Bureau of Reclamation. (2014) https://www.usbr.gov/gp/otao/estimating_cost_brackish_groundwater_desalination_texas.pdf.

Stumm, W., J.J. Morgan. *Water Chemistry: Chemical Equilibria and Rates in Natural Waters*. 3rd ed. New York, NY: John Wiley & Sons, (1996) 1022 p. ISBN 0-471-51184-6.

Talaat, H.A., Sorour, M.H., Abulnour, A.G., Shaalan, H.F. The Potential Role of Brackish Water Desalination Within the Egyptian Water Supply Matrix. Desalination 152, (2003), 375–382. https://doi.org/10.1016/S0011-9164(02)01086-X

Tandukar, S. "Recovery of Gypsum & Magnesium Hydroxide from Brackish Water by Chemical Precipitation." M.S. Thesis, University of New Mexico, Albuquerque, NM,. (2019), https://digitalrepository.unm.edu/ce_etds/238.

Thomson, B.M., K.J.Howe, , A., Shahi, , S. Tandukar, Mineral Recovery Enhanced Desalination (MRED) Process for Desalination and Recovery of Commodity Minerals, patent application, University of New Mexico, Albuquerque, NM (2019).

Thomson, B.M., K.J. Howe,. Saline Water - Considerations for Future Supply in New Mexico, In *Water, Natural Resources, and the Urban Landscape: The Albuquerque Region*, (2009),

pp. 120–126. Decision-Makers Field Conference Socorro, NM: N.M. Bureau of Mines & Mineral Resources.

Turek, M., W. Gnot,. Precipitation of Magnesium Hydroxide from Brine. Industrial and Engineering Che*mistry Research*, *34*(1), (1995), pp. 244–250. https://doi.org/10.1021/ie00040a025

TWDB.. The Future of Desalination in Texas, 2018 Biennial Report on Seawater and Brackish Groundwater Desalination. Austin, TX: Texas Water Development Board, (2018),https://www.twdb.texas.gov/innovativewater/desal/doc/2018_TheFutureofDesalinationinTexas.pdf?d=1546638725773.

Yuan, Q., Z. Lu, P. Zhang, X. Luo, X/ Ren, T. Golden.. Study of the Synthesis and Crystallization Kinetics of Magnesium Hydroxide. Materials Chemistry and Physics 162, (2015), 734–742. https://doi.org/doi.org/10.1016/j.matchemphys.2015.06.048

Ziolkowska, J.R., R. Reyes. Prospects for Desalination in the United States - Experiences from California, Florida, and Texas, Chapter 3.1.3. In *Competition for Water Resources: Experiences and Management Approaches in the U.S. and Europe*, Amsterdam: Elsevier, (2017), pp. 298-316. https://doi.org/10.1016/B978-0-12-803237-4.00017-3

Acknowledgments

This project was conducted with support from the Office of Fossil Energy of the U.S. Department of Energy's National Energy Technology Laboratory under federal grant award number DE-FE0030584. Mr. Atlin Johnson, an undergraduate student in the Department of Civil, Construction, and Environmental Engineering at the University of New Mexico, provided laboratory support. Dr. Abdulmehdi Ali, Research Scientist and manager of the Geoenvironmental Chemical Analysis Laboratory in the Department of Earth and Planetary Sciences at UNM provided extraordinary assistance with chemical analyses of lab samples. Mike Spilde in the Department of Earth and Planetary Sciences at UNM provided assistance with the electron microscopy. Dr. Eric Peterson in the Department of Earth and Planetary Sciences at UNM performed all of the X-ray analyses.

6 Author Contributions

Bruce Thomson – Conceptualization, Funding acquisition, Investigation, Methodology, Project Administration, Software, Supervision, Writing – original draft

Sugam Tandukar – Investigation, Methodology, Writing – review and editing

Ayush Shahi – Investigation, Methodology, Writing – review and editing

Carson Lee – Supervision, Writing – review and editing

Kerry Howe - Conceptualization, Funding acquisition, Investigation, Methodology, Project Administration, Supervision, Writing – review and editing

7 Appendix I – Solubility Calculations for Different Ionic Strengths

The Truesdell-Jones equation was used to calculate individual ion activity coefficients (γ_i) for charged ions in solution as shown in Fig. 2. This equation is valid up to an ionic strength (I) of 2.5 M (Benjamin, 2015; Langmuir, 1997). The equation is:

$$log\ \gamma_i = - \frac{A\ z_i^2 \sqrt{I}}{1 + Ba\sqrt{I}} + bI \qquad (A.1)$$

A and *B* are constants from the Debye-Hückel theory with values of 0.509 and 0.3286 respectively. The values for the constants *a* and *b* are related to the size of each ion. The values used to prepare Fig. 2 are shown in Table A.1 (Langmuir, 1997).

Table A.1. Values of the a and b constant used in the Truesdell-Jones equation to calculate single ion activity coefficients

Cation	a	b	Anion	a	b
Na^+	4.32	0.06	Cl^-	3.71	0.01
Ca^{2+}	4.86	0.15	SO_4^{2-}	5.31	-0.07
Mg^{2+}	5.46	0.22			

The solubility products used to prepare Fig. 3 were obtained from Stumm and Morgan (1996). The values are summarized in Table A.2.

Table A.2. Reactions and values of solubility products used to calculate solubility of selected solid phases (Stumm and Morgan, 1996).

Solubility Reaction	Log K
$CaSO_4{\cdot}2H_2O_{(s)} = Ca^{2+} + SO_4^{2-} + 2H_2O$	-4.58
$Mg(OH)_{2(s)} + 2H^+ = Mg^{2+} + 2H_2O$	16.84
$CaCO_{3(s)} = Ca^{2+} + CO_3^{2-}$	-8.48
$SiO_{2(am)} + 2H_2O = Si(OH)_4°$	-2.71